Immunity
Article

Virus Recognition by Toll-7 Activates Antiviral Autophagy in *Drosophila*

Margaret Nakamoto,[1,2] Ryan H. Moy,[1,2] Jie Xu,[1] Shelly Bambina,[1] Ari Yasunaga,[1] Spencer S. Shelly,[1] Beth Gold,[1] and Sara Cherry[1,*]
[1]Department of Microbiology, Penn Genome Frontiers Institute, University of Pennsylvania School of Medicine, Philadelphia, PA 19104, USA
[2]These authors contributed equally to this work
*Correspondence: cherrys@mail.med.upenn.edu
DOI 10.1016/j.immuni.2012.03.003

SUMMARY

Innate immunity is highly conserved and relies on pattern recognition receptors (PRRs) such as Toll-like receptors (identified through their homology to *Drosophila* Toll) for pathogen recognition. Although *Drosophila* Toll is vital for immune recognition and defense, roles for the other eight *Drosophila* Tolls in immunity have remained elusive. Here we have shown that Toll-7 is a PRR both in vitro and in adult flies; loss of Toll-7 led to increased vesicular stomatitis virus (VSV) replication and mortality. Toll-7, along with additional uncharacterized *Drosophila* Tolls, was transcriptionally induced by VSV infection. Furthermore, Toll-7 interacted with VSV at the plasma membrane and induced antiviral autophagy independently of the canonical Toll signaling pathway. These data uncover an evolutionarily conserved role for a second *Drosophila* Toll receptor that links viral recognition to autophagy and defense and suggest that other *Drosophila* Tolls may restrict specific as yet untested pathogens, perhaps via non-canonical signaling pathways.

INTRODUCTION

Detection and clearance of viruses by the innate immune system involves several distinct and essential pathways that are evolutionarily conserved (Janeway and Medzhitov, 2002). These pathways rely on pattern recognition receptors (PRRs) to recognize pathogen-associated molecular patterns (PAMPs), molecular signatures shared by wide classes of invading organisms, and induce an appropriate effector response to clear the infection. One important class of PRRs are the Toll-like receptors (TLRs), which were first identified in *Drosophila* through their homology to Toll, and are now recognized as the canonical pathogen recognition system in all metazoans (Uematsu and Akira, 2006).

Drosophila encodes nine Toll receptors (Bilak et al., 2003). The first to be identified, Toll, is the upstream receptor for the Toll pathway, which is the main defense against Gram-positive bacterial and fungal infections and is conserved in many insects (Cerenius et al., 2010; Lemaitre and Hoffmann, 2007; Lemaitre et al., 1996). These microbes are sensed by a variety of recognition molecules that activate a proteolytic cascade converging on the activation of spätzle, a cytokine that binds to Toll thereby inducing an NF-κB-dependent transcriptional program for antimicrobial defense. Surprisingly, a role for the additional eight *Drosophila* Toll homologs in innate immune defense has yet to be established. Toll-2 (18-wheeler) may have a minor role in the antibacterial response (Ligoxygakis et al., 2002; Williams et al., 1997), and Toll-5 (Tehao) and Toll-9 can activate the expression of the antifungal gene *Drosomycin* (Bilak et al., 2003; Luo et al., 2001; Ooi et al., 2002; Tauszig et al., 2000). However, these receptors have not been implicated as essential components of the immune response or in the recognition of any pathogen (Narbonne-Reveau et al., 2011; Yagi et al., 2010).

In contrast to *Drosophila*, studies have quickly identified a role for the ten human TLRs in immunity. Mutants in the TLRs are more susceptible to infection, and the PAMPs recognized by TLRs have been well characterized. Viral nucleic acids are recognized via endolysosomal TLRs (TLRs 3, 7, 8, 9) and viral glycoproteins can be recognized by TLRs present on the cell surface (e.g., TLR4) (Akira et al., 2006; Kawai and Akira, 2006). Unlike the indirect recognition of microbes by Toll, the mammalian TLRs generally bind microbial PAMPs directly to activate innate immune effectors (Jin and Lee, 2008).

One such effector pathway is autophagy, which can be induced by TLR signaling, although its in vivo significance is unknown (Delgado et al., 2009; Xu and Eissa, 2010). Autophagy is an ancient and conserved pathway that degrades intracellular components and can restrict a variety of intracellular pathogens, including viruses (Deretic and Levine, 2009; Lee et al., 2007; Levine et al., 2011; McPhee and Baehrecke, 2009). In *Drosophila*, autophagy is triggered upon recognition of the vesicular stomatitis virus (VSV) glycoprotein VSV-G, and this pathway is essential for antiviral defense in adult flies (Shelly et al., 2009). The response can be activated by viral recognition independently of viral replication, and therefore we hypothesized that VSV might be recognized by a *Drosophila* PRR controlling antiviral autophagy. Because the TLRs are known PRRs and VSV-G was previously shown to induce TLR4 signaling in mammalian cells (Georgel et al., 2007), we reasoned that one of the nine *Drosophila* Tolls could be the PRR linking viral recognition to this innate immune response. By screening mutants in the nine *Drosophila* Tolls in both cells and adult flies, we found that VSV was recognized by Toll-7, which restricted viral replication and thereby protected flies from an otherwise lethal infection. Toll-7 interacted with VSV virions at the plasma membrane, and this recognition was required for the induction of antiviral autophagy.

Together, these data demonstrate that pathogen recognition by *Drosophila* Tolls may be more similar than previously assumed to the mammalian systems and that there may be unknown roles for the additional Tolls in antiviral defense.

RESULTS

Toll-7 Restricts VSV Infection in Cultured Cells

To determine whether any of the *Drosophila* Tolls are involved in antiviral defense against VSV, we generated double-stranded RNA (dsRNA) against each of the nine Toll receptors and depleted them in *Drosophila* S2 cells via RNA interference (RNAi). Efficient silencing for each Toll receptor was confirmed by reverse transcriptase-polymerase chain reaction (RT-PCR) (Figure S1 available online). Next, we challenged RNAi-treated cells with VSV-GFP and subsequently analyzed the infection by fluorescence microscopy and automated image analysis. We observed an increase in the percentage of infected cells upon silencing of Toll-7 and Toll-2 but not other Tolls (Figures 1A and 1B). This increase was similar to that observed upon silencing of Atg8, an essential autophagy protein. Immunoblot analysis further confirmed that there was an elevation in the amount of GFP production in cells depleted of Toll-7 or Toll-2 but not other Toll receptors (Figure 1C, not shown). Interestingly, Toll-7 and Toll-2 are highly similar, showing 61% identity and 74% similarity, and are located in close chromosomal proximity (250 kb apart). Taken together, our data suggest that Toll-7 and Toll-2 might represent a gene duplication and play a similar antiviral role in vivo (Yagi et al., 2010).

Toll-7 Is Essential for Antiviral Defense in Adult Flies

Because *Drosophila* Toll-7 and Toll-2 were antiviral in vitro, we next investigated whether these receptors or any of the other Tolls play similar innate antiviral roles in the adult organism. With in vivo RNAi, we screened these genes to determine whether loss of any of these factors had an effect on VSV replication. Toll receptor-depleted flies were generated by driving expression of transgenes bearing long hairpin double-stranded RNA constructs targeting each Toll gene (Dietzl et al., 2007). For *Toll* (*Tl*) and *Toll-4* through *Toll-9*, we crossed control and transgenic flies to a strong ubiquitous driver, Actin-GAL4, to constitutively express the transgene. Because the *Toll-2* (*18w*) and *Toll-3* (*Mstprox*) transgenes were lethal when driven ubiquitously during development, we crossed them to heat-shock-GAL4 to allow for inducible transgene expression. Once again, silencing of each Toll was confirmed, although we were unable to detect Toll-3 and Toll-4 expression (Figure S2A). Silenced flies along with their sibling controls were challenged with VSV and monitored for changes in viral infection at day 6 postinfection. Only the loss of Toll-7 had a significant effect on VSV infection and led to an increase in viral RNA production (Figure 2A). Furthermore, increased viral replication upon Toll-7 depletion was also observed at day 9 postinfection (Figure 2B). To validate the Toll-7 phenotype, we challenged a second independent transgenic RNAi line and similarly found that silencing of Toll-7 resulted in increased VSV replication as measured by RNA blot at day 6, as well as at later time points (Figures S2B and S2C). Finally, adult flies expressing heat shock-driven Toll-7 dsRNA exhibited increased viral replication, suggesting that the susceptibility of Toll-7-depleted flies to VSV infection is not due to developmental defects (Figure S2D).

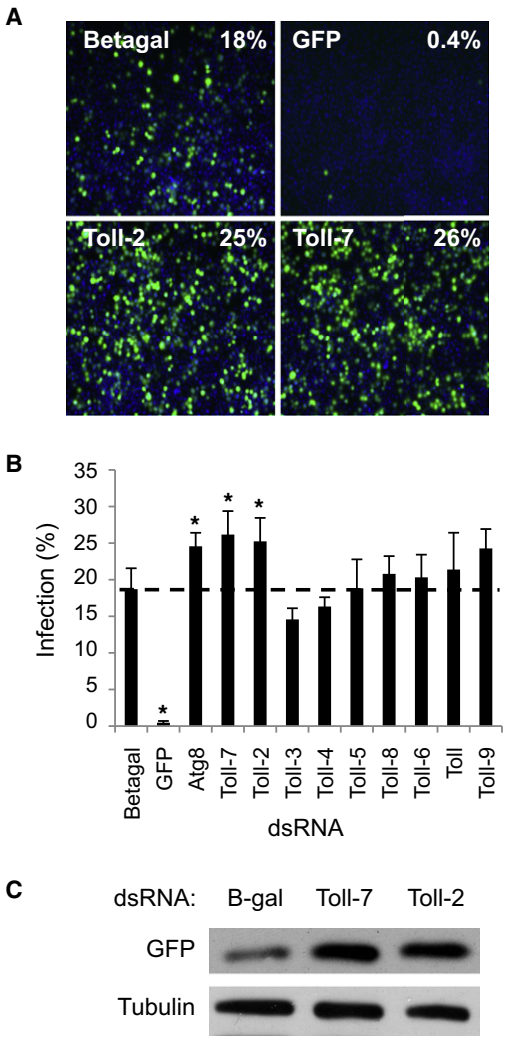

Figure 1. *Drosophila* Toll-7 and Toll-2 Are Antiviral in Cells

(A) *Drosophila* cells pretreated with dsRNAs against the indicated genes were infected with VSV (MOI = 0.1) for 20 hr and processed for immunofluorescence. Infected cells express GFP, and the percent infection is calculated with automated image analysis (MetaXpress) from three wells, with three sites per well (virus, green; nuclei, blue).

(B) Percent infection for three experiments is shown; mean ± SE, *$p < 0.01$, Student's t test.

(C) Cells pretreated with the indicated dsRNAs were infected (MOI = 0.1) and processed for immunoblot 20 hr p.i.; a representative experiment of three is depicted.

Because RNAi-mediated silencing is incomplete and Toll-2 was antiviral in cell culture (Figure 1), we tested whether previously characterized *Toll-2* mutant flies ($18w^{\Delta 7\text{-}35/Df(2R)017}$) were more susceptible to VSV infection (Ligoxygakis et al., 2002). In contrast to our in vitro results, Toll-2 was dispensable for defense against VSV in adult flies (Figure S2E). Taken together, these data suggest that Toll-7 but not Toll-2 is an essential component of the antiviral arsenal in both cells and adult flies.

Next, we evaluated whether Toll-7 depletion alters the susceptibility of flies to VSV infection. Depletion of Toll-7 had no effect

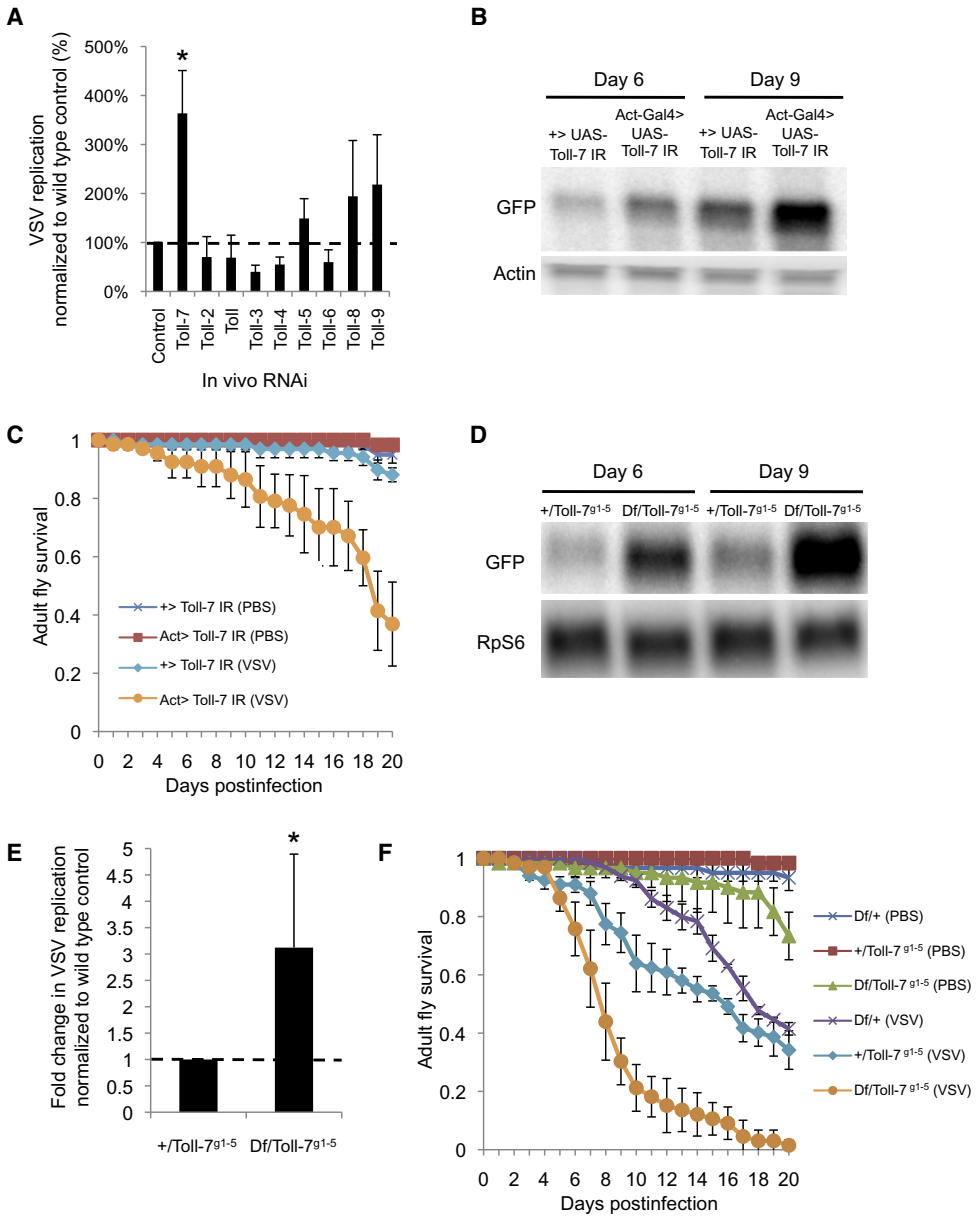

Figure 2. Toll-7 Is Antiviral in Adult Flies

(A) Adult flies expressing dsRNA against the indicated Toll receptors and their sibling controls were challenged with VSV and monitored for viral replication at 6 days p.i. by RNA blot and quantified relative to a cellular control mRNA (Actin). Fold change of the mean ± SD compared to sibling controls for three experiments is shown; *$p < 0.05$, Student's t test.

(B) Toll-7-depleted flies (Actin-Gal4 > UAS-Toll-7 IR) or sibling controls (+ > UAS-Toll-7 IR) were challenged with VSV and viral RNA was monitored by RNA blot at the indicated time points p.i. A representative blot is depicted; results were repeated in at least three experiments.

(C) Adult flies expressing dsRNA against Toll-7 (Actin-Gal4 > UAS-Toll-7 IR) or sibling controls (+ > UAS-Toll-7 IR) were challenged with vehicle (PBS) or VSV, and morbidity was monitored as a function of time after infection. Mean ± SE is shown for three experiments (Log-rank test, $p < 0.02$).

(D) *Toll-7* mutant (Df(2R)BSC22/Toll-7^{g1-5}) or control (+/Toll-7^{g1-5}) flies were infected with VSV and viral replication was monitored by RNA blot.

(E) Average fold change of viral RNA in *Toll-7* mutants compared to controls normalized to *RpS6* expression at 6 days p.i.; mean ± SD; *$p < 0.05$, Student's t test.

(F) Survival of VSV-challenged *Toll-7* mutant (Df(2R)BSC22/Toll-7^{g1-5}) or sibling control (Df(2R)BSC22/+ and +/Toll-7^{g1-5}) flies for three experiments (mean ± SE; Log-rank test, $p < 0.001$).

on the lifespan of adult flies (Figure 2C). We challenged control (+ > UAS-Toll-7 IR) or Toll-7-depleted (Actin-GAL4 > UAS-Toll-7 IR) flies with VSV and found that whereas the control flies were viable, the Toll-7-depleted flies succumbed to infection (Figure 2C). Thus, Toll-7 depletion in adult flies promotes increased viral replication, leading to mortality from an otherwise nonlethal infection.

Although silenced flies exhibited decreased Toll-7 mRNA expression, RNAi carries potential caveats such as driver over-expression and off-target silencing. To address these concerns,

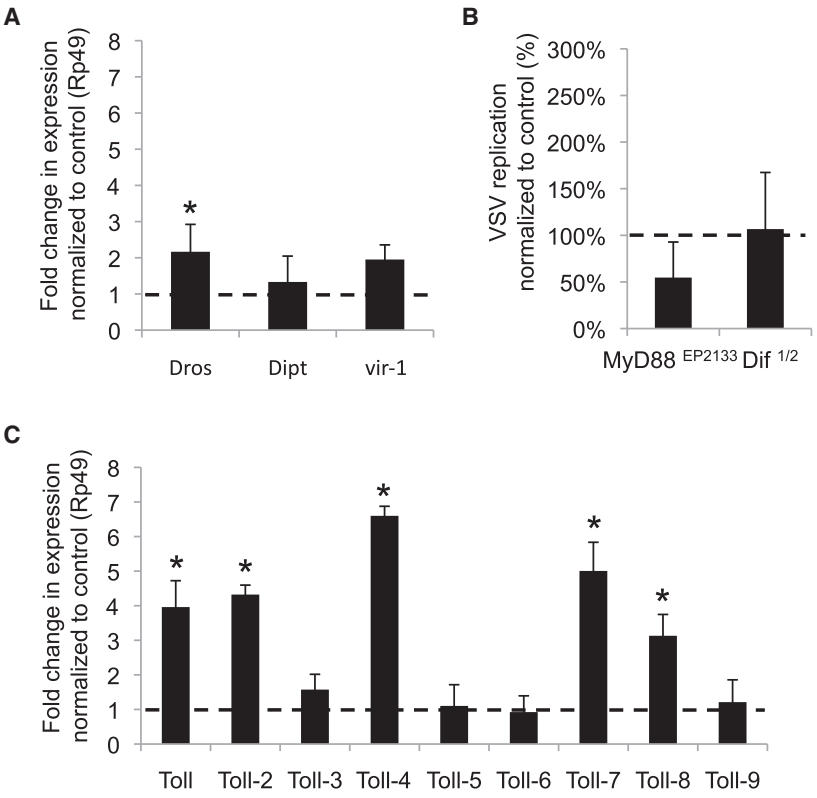

Figure 3. Toll-7, but Not the Canonical Innate Immune Signaling Pathways, Is Transcriptionally Induced by VSV Infection

(A) *Drosophila* cells were either uninfected or infected with VSV for 4 hr and processed for RT-qPCR of the Toll pathway AMP *Drosomycin*, the Imd pathway AMP *Diptericin*, and the Jak-Stat pathway readout *vir-1*. These were normalized to a control gene (*Rp49*) and fold change of mean ± SD for three experiments is shown; *$p < 0.01$, Student's t test.

(B) Adult flies either heterozygous or homozygous mutant for the Toll pathway components MyD88 and the NF-κB transcription factor Dif were challenged with VSV and viral replication was monitored by RNA blot at 6 days p.i. and quantified relative to a cellular control (Actin). Fold change compared to heterozygous control of the mean ± SD for three experiments is shown.

(C) Expression of the *Drosophila* Tolls from VSV-infected cells 4 hr p.i. compared to uninfected cells was analyzed by RT-qPCR; mean ± SD, *$p < 0.01$, Student's t test.

we obtained a recently reported *Toll-7* mutant fly line harboring a deletion in the *Toll-7* coding region (Toll-7^{g1-5}) (Yagi et al., 2010). These flies were crossed to a deficiency strain to generate flies lacking Toll-7 expression, and we confirmed the deletion at the DNA level by genotyping and at the RNA level by RT-PCR (Figures S2F–S2H). *Toll-7* mutants and control flies were infected with VSV, and consistent with the in vivo RNAi results, the *Toll-7* mutants demonstrated significantly elevated viral replication (Figures 2D, 2E, and S2I). This increased viral RNA load correlated with decreased survival of the *Toll-7* mutants after infection (Figure 2F). Collectively, these data further verify Toll-7 as a critical antiviral factor against VSV in vivo.

VSV Infection Induces Toll-7 Expression but Not Other Canonical Signaling Pathways

Drosophila has evolved multiple pathways to defend against invading pathogens, among which are the Toll, IMD, and Jak-Stat pathways (Lemaitre and Hoffmann, 2007; Sabin et al., 2010). Each of these pathways responds to different invading pathogens and ultimately leads to the induction of specific antimicrobial peptides (AMPs) (Lemaitre and Hoffmann, 2007). Because all the *Drosophila* Tolls have a conserved Toll and Interleukin-1 receptor (TIR) domain (Imler and Zheng, 2004), we explored whether Toll-7 signals via the canonical Toll signaling pathway. The Toll-dependent AMP gene *Drosomycin* is potently activated after fungal infection, but it was only modestly induced by VSV infection in cultured cells (~2-fold; Figure 3A). To examine whether this induction reflects a requirement for the Toll signaling pathway in restricting VSV infection in vivo, we challenged flies mutant for canonical pathway components including the TIR adaptor MyD88 and NF-κB member Dif, both of which are essential for fungal and Gram-positive bacterial immunity in adult flies (Bilak et al., 2003; Ip et al., 1993; Tauszig-Delamasure et al., 2002). Loss of these critical Toll pathway components had no impact on VSV replication in vivo, suggesting that Toll-7 signals through a distinct pathway (Figure 3B).

The IMD pathway is also activated by a PRR and converges on alternative NF-κB transcription factors that induce a different spectrum of AMPs including *Diptericin* (Lemaitre and Hoffmann, 2007). We also explored this pathway to see whether Toll-7 might be signaling through downstream members and found that VSV infection did not affect *Diptericin* expression in cell culture (Figure 3A).

Lastly, we examined the Jak-Stat signaling pathway, which has been shown to play antiviral roles in both flies and mammals (Dostert et al., 2005; García-Sastre and Biron, 2006). Upon VSV infection of cells, we found that expression of *vir-1*, a virus-specific Stat-dependent gene in *Drosophila*, was unperturbed (Figure 3B). These data suggest that Toll-7 mediates its antiviral effects through a signaling cascade distinct from the canonical Toll, IMD, or Jak-Stat pathways.

Many genes with roles in immunity are regulated by infection, so we examined the expression of Toll-7 (and the other Toll receptors) after VSV infection. Cells were challenged with VSV, and Toll-7 along with Toll, Toll-2, Toll-4, and Toll-8 were transcriptionally induced, indicating a potential role for these genes in immunity (Figure 3C).

Toll-7 Is a Surface Receptor that Interacts with VSV

TLRs can reside either at the plasma membrane or within endosomal compartments where they interact directly or indirectly with pathogens. Therefore, we characterized the subcellular localization of Toll-7. For these studies we generated an antibody that recognizes endogenous Toll-7 and found that RNAi

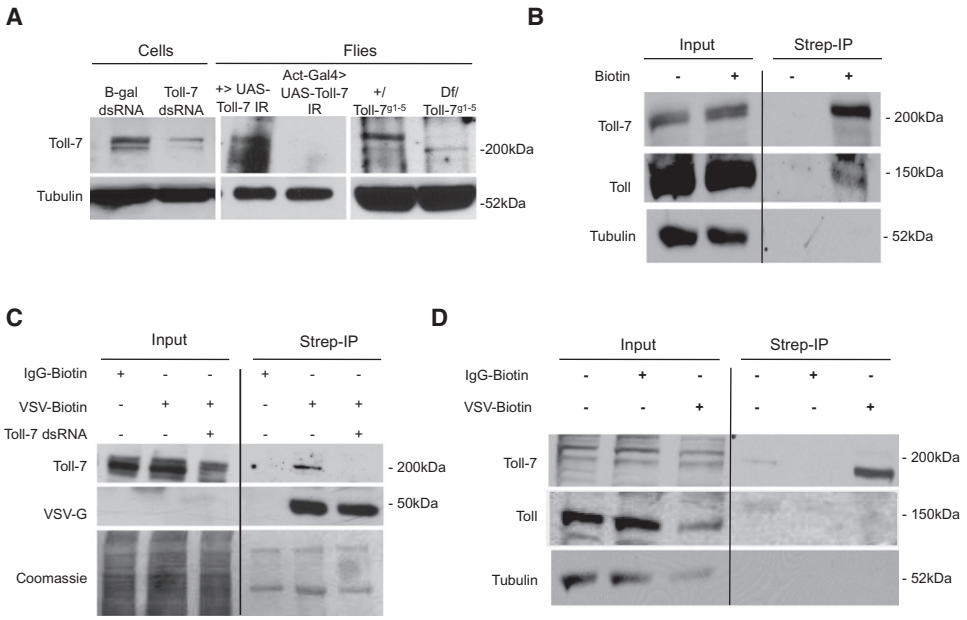

Figure 4. Toll-7 Is a Membrane-Bound Receptor that Interacts with VSV

(A) Immunoblot of *Drosophila* cells treated with control or Toll-7 dsRNA (left), adult flies expressing dsRNA against Toll-7 (Actin-Gal4 > UAS-Toll-7 IR), or sibling controls (+ > UAS-Toll-7 IR) (center) and *Toll-7* mutant (Df(2R)BSC22/Toll-7^{g1-5}) or control (+/Toll-7^{g1-5}) flies (right) probed for Toll-7 and control (tubulin). A representative experiment is shown; similar findings were made in at least three experiments.

(B) Cells at 4°C were left untreated or biotinylated for 1 hr, and lysates were probed with the indicated antibodies (input, left; precipitate, right). A representative experiment is shown; similar findings were made in at least three experiments.

(C) *Drosophila* cells treated with the indicated dsRNA were left untreated or incubated with biotinylated IgG or biotinylated VSV for 1 hr at 4°C. Lysates were precipitated with streptavidin beads and immunoblotted for Toll-7 or VSV-G. Coomassie staining is shown as a loading control. A representative experiment is shown; similar findings were made in at least three experiments.

(D) Cells were left untreated or incubated with biotinylated VSV for 1 hr at 4°C. Lysates were precipitated with streptavidin beads and immunoblotted with the indicated antibodies. A representative experiment is shown; similar findings were made in at least three experiments.

against Toll-7 efficiently depleted the protein in both cells and flies (Figure 4A). Toll-7 protein was also undetectable in the *Toll-7* mutant flies (Figure 4A), and transgenic flies expressing *Toll-7* under control of heat-shock-GAL4 exhibited increased Toll-7 protein, further validating the antibody's activity (Figure S3). To test whether Toll-7 is a plasma membrane-resident protein, we surface biotinylated *Drosophila* cells with a cell-impermeable form of biotin and precipitated the biotinylated proteins with avidin. Similar to the known surface-resident protein Toll, Toll-7 was precipitated by avidin whereas tubulin, an intracellular protein, was not found in the precipitate (Figure 4B).

In general, mammalian TLRs bind directly to their PAMPs, whereas recognition by *Drosophila* Toll is indirect. Toll is instead activated by the cytokine spätzle, which is the product of a proteolytic cascade induced upon upstream recognition of bacterial and fungal PAMPs (Akira et al., 2006; Ferrandon et al., 2004; Lemaitre et al., 1996). Therefore, we tested whether VSV interacted with Toll-7 at the cell surface. Cells were pre-bound with purified biotinylated infectious VSV at 4°C to allow for surface binding. After 1 hr, unbound virus was removed and cell lysates were applied to avidin beads. Precipitation of proteins bound to VSV revealed that VSV-G was efficiently precipitated, as indicated by the fact that we were unable to detect the low amount in the input (Figure 4C). We found that VSV interacted with endogenous Toll-7 at the plasma membrane and that this interaction was lost upon RNAi depletion of Toll-7 (Figure 4C). Moreover, the interaction between Toll-7 and VSV was specific, as indicated by the fact that Toll-7 did not bind biotinylated IgG (Figures 4C and 4D). Lastly, whereas Toll-7 precipitated with VSV, the plasma membrane protein Toll and the intracellular protein tubulin did not precipitate, suggesting that Toll-7 is a specific and bona fide PRR for VSV (Figure 4D).

VSV-Induced Autophagy Is Dependent on Toll-7 in Cultured Cells

Because both Toll-7 and autophagy show similar antiviral activity against VSV, we tested whether Toll-7 is the PRR upstream of autophagy. In order to examine autophagy, we implemented a commonly used assay dependent upon the change in localization of an expressed GFP-tagged Light Chain 3 (GFP-LC3) in *Drosophila* cells (Juhasz and Neufeld, 2008; McPhee et al., 2010; Rusten et al., 2004; Shelly et al., 2009). Under normal conditions, LC3 shows diffuse cytoplasmic staining; however, it is translocated to autophagosomes when autophagy is induced, appearing as bright puncta within the cell (Klionsky et al., 2008; Mizushima et al., 2010). Upon VSV infection or starvation, we observed a significant increase in the number of LC3 puncta per cell compared to control cells (Figures 5A–5C; quantified in Figures 5D and S4). This induction was dependent on canonical autophagy proteins, as shown by the fact that depletion of Atg5, a core component of this pathway, blocked the

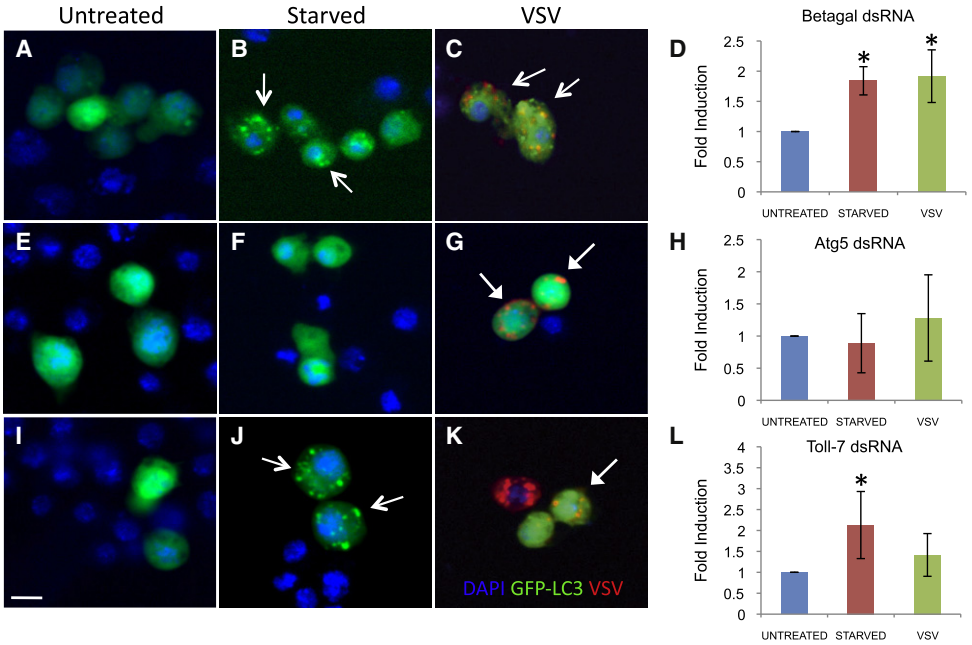

Figure 5. Toll-7 Is Required for Antiviral Autophagy in Cell Culture

Cells transfected with a GFP-LC3 reporter (green) were treated with dsRNA against a negative control (Betagal) (A, B, C), canonical autophagy component Atg5 (E, F, G), or Toll-7 (I, J, K). Cells were left uninfected (A, E, I), starved (B, F, J), or infected with VSV for 22 hr (MOI = 10) (C, G, K). Representative images are shown (nuclei, blue; GFP-LC3, green; VSV-G, red). Open arrows indicate GFP-LC3$^+$ puncta and closed arrows indicate VSV$^+$ cells devoid of GFP-LC3 puncta. Scale bar represents 10 μm. Quantification of the fold change (D, H, L) in puncta per cell for triplicate experiments; mean ± SD is shown; *$p < 0.02$, Student's t test.

puncta formation induced by either VSV infection or starvation (Figures 5E–5G; quantified in Figures 5H and S4). In contrast, upon silencing of Toll-7, VSV-induced puncta were lost whereas starvation-induced puncta were unaffected (Figures 5I–5K; quantified in Figures 5L and S4). Taken together, these results indicate that Toll-7 is specifically required for antiviral autophagy but is dispensable for starvation-induced autophagy.

Toll-7 Mediates the Antiviral Autophagy Response in Adult Flies

Next, we evaluated whether Toll-7 is required for VSV-induced autophagy in vivo. To examine autophagy in adult flies, we used a well-characterized assay that takes advantage of Lysotracker, a marker of acidified compartments, to observe the induction of late-stage autophagosomes in the fat body, which lacks an acidic pH under normal conditions (Arsham and Neufeld, 2009; Bilen and Bonini, 2007; Chen et al., 2008; McPhee et al., 2010; Rusten et al., 2004; Shelly et al., 2009). Toll-7-silenced flies or sibling controls were infected with VSV-GFP and dissected 3 days after infection, at which time the fat body was removed and stained with Lysotracker. Although control flies showed significant Lysotracker staining in VSV-infected fat body cells, Toll-7-depleted flies exhibited minimal Lysotracker staining despite extensive viral infection, as monitored by GFP expression (Figure 6A, quantified in Figure 6B). Uninfected Toll-7-silenced flies or sibling controls had little Lysotracker staining of fat body cells (data not shown).

To further verify that Toll-7 is required for the induction of autophagy downstream of VSV infection in adult flies, we implemented an immunoblot assay. During autophagy, cytosolic LC3 (LC3-I or Atg8-I) is conjugated with phosphatidylethanolamine, forming a lipidated form of LC3 (LC3-II or Atg8-II) that decorates the autophagic membrane and results in a size shift by immunoblot (Shelly et al., 2009). Control flies exhibited a strong induction of autophagy after VSV infection as monitored by increased Atg-II amounts; however, VSV-activated autophagy was severely abrogated in Toll-7-depleted flies (Figure 6C). Consistent with these results, *Toll-7* mutant flies demonstrated a reduction in Atg8-II production after VSV challenge compared to the controls (Figure 6D). Autophagy was induced independently of canonical Toll signaling as shown by the fact that *Myd88* mutant flies showed substantial Atg8-II accumulation after VSV infection (Figure S5). Together, our results confirm that Toll-7 is required for VSV-induced antiviral autophagy both in vitro and in vivo.

DISCUSSION

The essential role for *Drosophila* Toll in antimicrobial defense is firmly established; however, whether other Toll receptors serve important immune functions has been poorly understood. We have identified a role for a second *Drosophila* Toll receptor, Toll-7, in antiviral defense both in cells and animals. Toll-7-depleted cells exhibited increased VSV infectivity, and Toll-7-deficient flies demonstrated significantly elevated viral replication and mortality after VSV challenge. Furthermore, Toll-7 acted as a PRR by interacting with VSV at the plasma membrane to induce an effector program that converged on antiviral

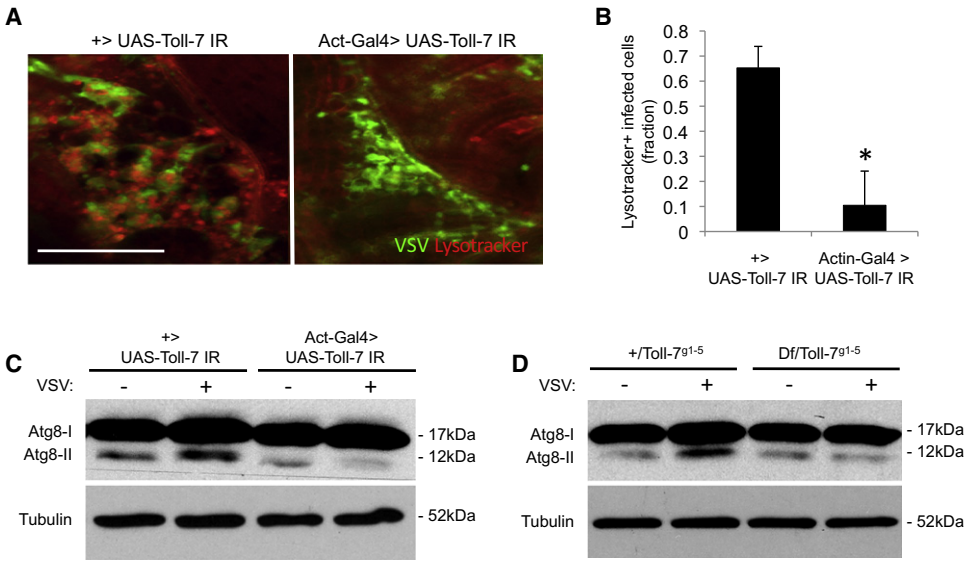

Figure 6. Toll-7 Is Required for Antiviral Autophagy in Adult Flies

(A) Control flies (+ > UAS-Toll-7 IR) or Toll-7-depleted flies (Actin-Gal4 > UAS-Toll-7 IR) were challenged with VSV-GFP for 3 days. The flies were monitored for infection (GFP^+) and autophagy ($Lysotracker^+$). Representative images of fat body demonstrate that autophagy is induced in infected wild-type cells but not in the infected Toll-7-depleted cells. Scale bar represents 100 μm.

(B) The percentage of virally infected cells (GFP^+) with puncta ($Lysotracker^+$) was quantified. Mean ± SD shown for three experiments; *$p < 0.0001$, Student's t test.

(C) Immunoblot of control flies (+ > UAS-Toll-7IR) or Toll-7-depleted flies (Actin-Gal4 > UAS-Toll-7 IR) challenged with VSV for 2 days. Autophagy was monitored by size shift of Atg8 (Atg8-II accumulation) and samples were normalized to the control protein tubulin. These data show representative experiments; similar findings were made in at least three experiments.

(D) Immunoblot of Atg8 expression from VSV-challenged *Toll-7* mutant (Df(2R)BSC22/Toll-7^{g1-5}) or control (+/Toll-7^{g1-5}) flies day 3 postinfection. A representative image of three experiments is presented.

autophagy. The function of Toll-7 appears to be specific to antiviral immunity, as shown by the fact that Toll-7-deficient flies mount appropriate AMP responses to septic injury (Yagi et al., 2010).

Multiple innate immune pathways in *Drosophila* rely on the activation of the transcription factor NF-κB; however, the Toll-7-dependent autophagy response is probably elicited via an NF-κB-independent mechanism. Unlike Toll-7-deficient flies, flies lacking core Toll pathway components did not demonstrate increased susceptibility to VSV. Moreover, the IMD pathway was not activated by viral infection. In agreement with these data, MyD88 was also not required for the induction of antiviral autophagy. This NF-κB independence is consistent with previous studies that found that the NF-κB-dependent AMPs *Diptericin* and *Drosomycin* are not induced in *Drosophila* cells when stimulated with a hyperactive form of Toll-7 (Tauszig et al., 2000) and that Toll-7 is dispensable for immunity to NF-κB-dependent bacterial challenges (Yagi et al., 2010). Hence, although Toll-7 probably activates noncanonical signaling pathways, the exact pathways downstream of Toll-7 remain to be determined.

Recent studies in mammals found that TLR activation can lead to the induction of autophagy in a variety of cultured cells (Delgado et al., 2008; Sanjuan et al., 2007; Shin et al., 2010; Xu et al., 2007). However, the mechanism by which TLR stimulation converges on autophagy is unclear. Moreover, the dependence on specific signaling molecules is controversial and whether TLR-induced autophagy is important in restricting infection in vivo is unknown (Delgado et al., 2009; Xu and Eissa, 2010). Our data, together with the findings that *Listeria* recognition via a peptidoglycan recognition protein induces autophagy (Yano et al., 2008), suggest that multiple classes of PRRs are involved in the induction of antimicrobial autophagy, which plays an important role in the control of a diverse set of pathogens.

Whereas the discovery of Toll as an innate immune receptor led to the identification of TLRs as a large family of PRRs, studies demonstrating a role for the additional eight Toll receptors in immunity have lagged behind. This discrepancy may be in part due to the lack of studies probing the role of the additional eight Toll receptors in antiviral defense. Perhaps the lack of classical cytoplasmic sensors (RIG-I and MDA5) has required *Drosophila* to be more heavily dependent on the Tolls for viral recognition, opening up the possibility that additional *Drosophila* Toll receptors play roles in antiviral immunity. This hypothesis is further supported by our finding that a number of uncharacterized Tolls are induced by viral infection similar to the two major antiviral TLRs, TLR3 and TLR7, which are transcriptionally induced by viral infection in mammalian systems (Sirén et al., 2005; Takeda et al., 2003). Importantly, Toll-7 is conserved in vector mosquitoes, suggesting that Toll-7 and other Toll receptors may be involved in the recognition and restriction of human arboviruses (Waterhouse et al., 2007).

TLRs are generally thought to directly bind their PAMPs, whereas *Drosophila* Toll functions indirectly by recognizing a host cytokine. Our findings that Toll-7 interacts with VSV virions

suggest that Toll-7 might act directly as a pattern recognition receptor more similar to mammalian TLRs, a previously unknown mechanism for an insect Toll receptor. Although VSV is an arbovirus, the natural vectors have been proposed to be biting insects such as sand flies and blackflies (Comer et al., 1990; Mead et al., 2004); nevertheless, for several reasons we believe that VSV is a bona fide ligand for *Drosophila* Toll-7. First, Toll-7 is highly conserved between insect species that have been sequenced (66% identity and 77% homology to *Aedes aegypti* Toll-7), indeed, more so than many other Toll receptors. Second, although nucleic acids have been well characterized as viral PAMPs, emerging evidence suggests that viral proteins including glycoproteins can also activate TLRs (Barbalat et al., 2009; Barton, 2007). Importantly, there are several examples of murine TLRs that recognize PAMPs from viruses that naturally do not infect mice. Humans are the natural host of measles virus, yet the viral hemagglutinin still activates mouse TLR2 (Bieback et al., 2002). Likewise, *Tlr2*$^{-/-}$ murine macrophages have reduced cytokine responses to hepatitis C virus core and NS3, as well as to human cytomegalovirus, despite the fact that both viruses are human viruses (Chang et al., 2007; Compton et al., 2003). Moreover, in mouse macrophages and myeloid dendritic cells, VSV-G activates an antiviral response dependent on TLR4, even though VSV does not normally infect mice in the wild (Georgel et al., 2007). These results are consistent with the idea that PAMPs are molecular signatures often conserved across wide groups of pathogens and not necessarily restricted to a single microbe. It is therefore not unexpected that TLRs (as well as Tolls) can recognize these structures even if they have not yet encountered that particular pathogen. Third, although the Rhabdovirus VSV does not normally infect fruit flies, the closely related Rhabdovirus sigma virus is a natural *Drosophila* pathogen (Fleuriet, 1988). The *Drosophila* sigma viruses phylogenetically cluster more closely to the vesiculoviruses than other groups of Rhabdoviruses (Longdon et al., 2010). Furthermore, although autophagy has not formally been shown to restrict sigma virus, flies deficient in *Drosophila* p62 (*ref(2)p*), which serves as an autophagy cargo receptor implicated in the clearance of Sindbis virus capsids and other pathogens, are more susceptible to infection (Contamine et al., 1989; Dru et al., 1993; Orvedahl et al., 2010). Given the relatedness of sigma virus to VSV, we posit that the Toll-7 ligand on VSV may be similar to that of a natural *Drosophila* pathogen.

Intriguingly, the interaction between Toll-7 and VSV suggests that other Toll receptors may recognize presently undefined ligands, including pathogen-derived molecules. Taken together with studies on Toll in microbial defense, our data suggest that Toll receptors probably evolved to recognize foreign microbes and elicit antimicrobial effector mechanisms, therefore uncovering an evolutionarily conserved intrinsic antiviral program that links pathogen recognition to autophagy, which may be amenable to therapeutic intervention.

EXPERIMENTAL PROCEDURES

Cells and Viruses

Drosophila S2 cells and BHK cells were grown and maintained as described (Shelly et al., 2009). VSV or VSV-eGFP was grown as described (Ramsburg et al., 2005).

RNAi and Infections

dsRNAs for RNAi were generated and used for RNAi as described (Cherry et al., 2005). Amplicons used are described at http://www.flyrnai.org. Three days after dsRNA bathing, cells were infected with the indicated viral innoculum and assayed at the indicated time point postinfection.

Immunofluorescence

Cells were processed for immunofluorescence as previously described (Shelly et al., 2009) and imaged with an automated microscope (ImageXpress Micro). Three wells per treatment with three sites per well were collected and quantified (MetaXpress). S2* cells were transfected with pMT-Gal4 and UAS-GFP-LC3 and infected with VSV as previously described (Shelly et al., 2009). More than 150 cells per treatment were counted for three independent experiments.

Immunoblotting, RNA Blots, qPCR, and Titers

Cells or flies were collected at the indicated time points and lysed in radioimmunoprecipitation assay (RIPA) buffer supplemented with a protease inhibitor cocktail (Boehringer) and blotted as previously described for immunoblots (Shelly et al., 2009). Cells or purified virus were biotinylated with Sulfo-NHS-LC-Biotin according to the manufacturer's protocol at 4°C (Thermo). For immunoprecipitations, samples were lysed in lysis buffer (20 mM Tris at pH 7.6, 150 mM NaCl, 2 mM EDTA, 10% glycerol, 1% Triton X-100, 1 mM DTT, and protease inhibitors) (Aggarwal et al., 2008). Protein lysates were precipitated with streptavidin-agarose and immunoblotted. For RNA blot, total RNA was purified by Trizol and analyzed as previously described (Shelly et al., 2009). qPCR was performed on DNase-treated total RNA that had been reverse transcribed with random primers.

Adult Infections

4- to 7-day-old adults of the stated genotypes were inoculated with vehicle or VSV-GFP as previously described (Shelly et al., 2009). Flies were processed at the indicated time point postinfection. For autophagy studies, flies were dissected in complete Schneider's media with Lysotracker red (Invitrogen), incubated for 10 min, rinsed in media, and mounted live for imaging (Leica) (Shelly et al., 2009).

SUPPLEMENTAL INFORMATION

Supplemental Information includes Supplemental Experimental Procedures and five figures and can be found with this article online at doi:10.1016/j.immuni.2012.03.003.

ACKNOWLEDGMENTS

We thank S. Ross, R. Doms, and M. Tudor for critical reading of the manuscript; the VDRC for Toll snapback transgenic flies; the TRiP at Harvard Medical School (NIH/NIGMS R01-GM084947) for providing transgenic RNAi fly stocks; Y. Yagi for *Toll-7* mutants; The Bloomington Stock center for other fly stocks; J. Rose for VSV-GFP; and R. Doms for VSV-G (I1) antibody. This work was supported by NIH grants T32AI007324 to R.H.M. and R01AI074951 and U54AI057168 to S.C. S.C. is a recipient of the Burroughs Wellcome Investigators in the Pathogenesis of Infectious Disease Award.

Received: May 3, 2011
Revised: January 24, 2012
Accepted: March 5, 2012
Published online: March 29, 2012

REFERENCES

Aggarwal, K., Rus, F., Vriesema-Magnuson, C., Ertürk-Hasdemir, D., Paquette, N., and Silverman, N. (2008). Rudra interrupts receptor signaling complexes to negatively regulate the IMD pathway. PLoS Pathog. *4*, e1000120.

Akira, S., Uematsu, S., and Takeuchi, O. (2006). Pathogen recognition and innate immunity. Cell *124*, 783–801.

Arsham, A.M., and Neufeld, T.P. (2009). A genetic screen in *Drosophila* reveals novel cytoprotective functions of the autophagy-lysosome pathway. PLoS ONE *4*, e6068.

Barbalat, R., Lau, L., Locksley, R.M., and Barton, G.M. (2009). Toll-like receptor 2 on inflammatory monocytes induces type I interferon in response to viral but not bacterial ligands. Nat. Immunol. *10*, 1200–1207.

Barton, G.M. (2007). Viral recognition by Toll-like receptors. Semin. Immunol. *19*, 33–40.

Bieback, K., Lien, E., Klagge, I.M., Avota, E., Schneider-Schaulies, J., Duprex, W.P., Wagner, H., Kirschning, C.J., Ter Meulen, V., and Schneider-Schaulies, S. (2002). Hemagglutinin protein of wild-type measles virus activates toll-like receptor 2 signaling. J. Virol. *76*, 8729–8736.

Bilak, H., Tauszig-Delamasure, S., and Imler, J.L. (2003). Toll and Toll-like receptors in *Drosophila*. Biochem. Soc. Trans. *31*, 648–651.

Bilen, J., and Bonini, N.M. (2007). Genome-wide screen for modifiers of ataxin-3 neurodegeneration in *Drosophila*. PLoS Genet. *3*, 1950–1964.

Cerenius, L., Kawabata, S., Lee, B.L., Nonaka, M., and Söderhäll, K. (2010). Proteolytic cascades and their involvement in invertebrate immunity. Trends Biochem. Sci. *35*, 575–583.

Chang, S., Dolganiuc, A., and Szabo, G. (2007). Toll-like receptors 1 and 6 are involved in TLR2-mediated macrophage activation by hepatitis C virus core and NS3 proteins. J. Leukoc. Biol. *82*, 479–487.

Chen, G.C., Lee, J.Y., Tang, H.W., Debnath, J., Thomas, S.M., and Settleman, J. (2008). Genetic interactions between *Drosophila melanogaster* Atg1 and paxillin reveal a role for paxillin in autophagosome formation. Autophagy *4*, 37–45.

Cherry, S., Doukas, T., Armknecht, S., Whelan, S., Wang, H., Sarnow, P., and Perrimon, N. (2005). Genome-wide RNAi screen reveals a specific sensitivity of IRES-containing RNA viruses to host translation inhibition. Genes Dev. *19*, 445–452.

Comer, J.A., Tesh, R.B., Modi, G.B., Corn, J.L., and Nettles, V.F. (1990). Vesicular stomatitis virus, New Jersey serotype: replication in and transmission by *Lutzomyia shannoni* (Diptera: Psychodidae). Am. J. Trop. Med. Hyg. *42*, 483–490.

Compton, T., Kurt-Jones, E.A., Boehme, K.W., Belko, J., Latz, E., Golenbock, D.T., and Finberg, R.W. (2003). Human cytomegalovirus activates inflammatory cytokine responses via CD14 and Toll-like receptor 2. J. Virol. *77*, 4588–4596.

Contamine, D., Petitjean, A.M., and Ashburner, M. (1989). Genetic resistance to viral infection: the molecular cloning of a *Drosophila* gene that restricts infection by the rhabdovirus sigma. Genetics *123*, 525–533.

Delgado, M.A., Elmaoued, R.A., Davis, A.S., Kyei, G., and Deretic, V. (2008). Toll-like receptors control autophagy. EMBO J. *27*, 1110–1121.

Delgado, M., Singh, S., De Haro, S., Master, S., Ponpuak, M., Dinkins, C., Ornatowski, W., Vergne, I., and Deretic, V. (2009). Autophagy and pattern recognition receptors in innate immunity. Immunol. Rev. *227*, 189–202.

Deretic, V., and Levine, B. (2009). Autophagy, immunity, and microbial adaptations. Cell Host Microbe *5*, 527–549.

Dietzl, G., Chen, D., Schnorrer, F., Su, K.C., Barinova, Y., Fellner, M., Gasser, B., Kinsey, K., Oppel, S., Scheiblauer, S., et al. (2007). A genome-wide transgenic RNAi library for conditional gene inactivation in *Drosophila*. Nature *448*, 151–156.

Dostert, C., Jouanguy, E., Irving, P., Troxler, L., Galiana-Arnoux, D., Hetru, C., Hoffmann, J.A., and Imler, J.L. (2005). The Jak-STAT signaling pathway is required but not sufficient for the antiviral response of *Drosophila*. Nat. Immunol. *6*, 946–953.

Dru, P., Bras, F., Dezélée, S., Gay, P., Petitjean, A.M., Pierre-Deneubourg, A., Teninges, D., and Contamine, D. (1993). Unusual variability of the *Drosophila melanogaster* ref(2)P protein which controls the multiplication of sigma rhabdovirus. Genetics *133*, 943–954.

Ferrandon, D., Imler, J.L., and Hoffmann, J.A. (2004). Sensing infection in *Drosophila*: Toll and beyond. Semin. Immunol. *16*, 43–53.

Fleuriet, A. (1988). Maintenance of a hereditary virus, the sigma virus, in populations of its host, *D. melanogaster*. In Evolutionary Biology, M.K. Hecht and B. Wallace, eds. (New York: Plenum Press).

García-Sastre, A., and Biron, C.A. (2006). Type 1 interferons and the virus-host relationship: a lesson in détente. Science *312*, 879–882.

Georgel, P., Jiang, Z., Kunz, S., Janssen, E., Mols, J., Hoebe, K., Bahram, S., Oldstone, M.B., and Beutler, B. (2007). Vesicular stomatitis virus glycoprotein G activates a specific antiviral Toll-like receptor 4-dependent pathway. Virology *362*, 304–313.

Imler, J.L., and Zheng, L. (2004). Biology of Toll receptors: lessons from insects and mammals. J. Leukoc. Biol. *75*, 18–26.

Ip, Y.T., Reach, M., Engstrom, Y., Kadalayil, L., Cai, H., González-Crespo, S., Tatei, K., and Levine, M. (1993). Dif, a dorsal-related gene that mediates an immune response in *Drosophila*. Cell *75*, 753–763.

Janeway, C.A., Jr., and Medzhitov, R. (2002). Innate immune recognition. Annu. Rev. Immunol. *20*, 197–216.

Jin, M.S., and Lee, J.O. (2008). Structures of the toll-like receptor family and its ligand complexes. Immunity *29*, 182–191.

Juhasz, G., and Neufeld, T.P. (2008). Experimental control and characterization of autophagy in *DrosInophila*. Methods Mol. Biol. *445*, 125–133.

Kawai, T., and Akira, S. (2006). TLR signaling. Cell Death Differ. *13*, 816–825.

Klionsky, D.J., Abeliovich, H., Agostinis, P., Agrawal, D.K., Aliev, G., Askew, D.S., Baba, M., Baehrecke, E.H., Bahr, B.A., Ballabio, A., et al. (2008). Guidelines for the use and interpretation of assays for monitoring autophagy in higher eukaryotes. Autophagy *4*, 151–175.

Lee, H.K., Lund, J.M., Ramanathan, B., Mizushima, N., and Iwasaki, A. (2007). Autophagy-dependent viral recognition by plasmacytoid dendritic cells. Science *315*, 1398–1401.

Lemaitre, B., and Hoffmann, J. (2007). The host defense of *Drosophila melanogaster*. Annu. Rev. Immunol. *25*, 697–743.

Lemaitre, B., Nicolas, E., Michaut, L., Reichhart, J.M., and Hoffmann, J.A. (1996). The dorsoventral regulatory gene cassette spätzle/Toll/cactus controls the potent antifungal response in *Drosophila* adults. Cell *86*, 973–983.

Levine, B., Mizushima, N., and Virgin, H.W. (2011). Autophagy in immunity and inflammation. Nature *469*, 323–335.

Ligoxygakis, P., Bulet, P., and Reichhart, J.M. (2002). Critical evaluation of the role of the Toll-like receptor 18-Wheeler in the host defense of *Drosophila*. EMBO Rep. *3*, 666–673.

Longdon, B., Obbard, D.J., and Jiggins, F.M. (2010). Sigma viruses from three species of *Drosophila* form a major new clade in the rhabdovirus phylogeny. Proc. Biol. Sci. *277*, 35–44.

Luo, C., Shen, B., Manley, J.L., and Zheng, L. (2001). Tehao functions in the Toll pathway in *Drosophila melanogaster*: possible roles in development and innate immunity. Insect Mol. Biol. *10*, 457–464.

McPhee, C.K., and Baehrecke, E.H. (2009). Autophagy in *Drosophila melanogaster*. Biochim. Biophys. Acta *1793*, 1452–1460.

McPhee, C.K., Logan, M.A., Freeman, M.R., and Baehrecke, E.H. (2010). Activation of autophagy during cell death requires the engulfment receptor Draper. Nature *465*, 1093–1096.

Mead, D.G., Howerth, E.W., Murphy, M.D., Gray, E.W., Noblet, R., and Stallknecht, D.E. (2004). Black fly involvement in the epidemic transmission of vesicular stomatitis New Jersey virus (Rhabdoviridae: Vesiculovirus). Vector Borne Zoonotic Dis. *4*, 351–359.

Mizushima, N., Yoshimori, T., and Levine, B. (2010). Methods in mammalian autophagy research. Cell *140*, 313–326.

Narbonne-Reveau, K., Charroux, B., and Royet, J. (2011). Lack of an antibacterial response defect in *Drosophila* Toll-9 mutant. PLoS ONE *6*, e17470.

Ooi, J.Y., Yagi, Y., Hu, X., and Ip, Y.T. (2002). The *Drosophila* Toll-9 activates a constitutive antimicrobial defense. EMBO Rep. *3*, 82–87.

Orvedahl, A., MacPherson, S., Sumpter, R., Jr., Tallóczy, Z., Zou, Z., and Levine, B. (2010). Autophagy protects against Sindbis virus infection of the central nervous system. Cell Host Microbe *7*, 115–127.

Ramsburg, E., Publicover, J., Buonocore, L., Poholek, A., Robek, M., Palin, A., and Rose, J.K. (2005). A vesicular stomatitis virus recombinant expressing granulocyte-macrophage colony-stimulating factor induces enhanced T-cell responses and is highly attenuated for replication in animals. J. Virol. *79*, 15043–15053.

Rusten, T.E., Lindmo, K., Juhász, G., Sass, M., Seglen, P.O., Brech, A., and Stenmark, H. (2004). Programmed autophagy in the *Drosophila* fat body is induced by ecdysone through regulation of the PI3K pathway. Dev. Cell *7*, 179–192.

Sabin, L.R., Hanna, S.L., and Cherry, S. (2010). Innate antiviral immunity in *Drosophila*. Curr. Opin. Immunol. *22*, 4–9.

Sanjuan, M.A., Dillon, C.P., Tait, S.W., Moshiach, S., Dorsey, F., Connell, S., Komatsu, M., Tanaka, K., Cleveland, J.L., Withoff, S., and Green, D.R. (2007). Toll-like receptor signalling in macrophages links the autophagy pathway to phagocytosis. Nature *450*, 1253–1257.

Shelly, S., Lukinova, N., Bambina, S., Berman, A., and Cherry, S. (2009). Autophagy is an essential component of *Drosophila* immunity against vesicular stomatitis virus. Immunity *30*, 588–598.

Shin, D.M., Yuk, J.M., Lee, H.M., Lee, S.H., Son, J.W., Harding, C.V., Kim, J.M., Modlin, R.L., and Jo, E.K. (2010). Mycobacterial lipoprotein activates autophagy via TLR2/1/CD14 and a functional vitamin D receptor signalling. Cell. Microbiol. *12*, 1648–1665.

Sirén, J., Pirhonen, J., Julkunen, I., and Matikainen, S. (2005). IFN-alpha regulates TLR-dependent gene expression of IFN-alpha, IFN-beta, IL-28, and IL-29. J. Immunol. *174*, 1932–1937.

Takeda, K., Kaisho, T., and Akira, S. (2003). Toll-like receptors. Annu. Rev. Immunol. *21*, 335–376.

Tauszig, S., Jouanguy, E., Hoffmann, J.A., and Imler, J.L. (2000). Toll-related receptors and the control of antimicrobial peptide expression in *Drosophila*. Proc. Natl. Acad. Sci. USA *97*, 10520–10525.

Tauszig-Delamasure, S., Bilak, H., Capovilla, M., Hoffmann, J.A., and Imler, J.L. (2002). *Drosophila* MyD88 is required for the response to fungal and Gram-positive bacterial infections. Nat. Immunol. *3*, 91–97.

Uematsu, S., and Akira, S. (2006). Toll-like receptors and innate immunity. J. Mol. Med. *84*, 712–725.

Waterhouse, R.M., Kriventseva, E.V., Meister, S., Xi, Z., Alvarez, K.S., Bartholomay, L.C., Barillas-Mury, C., Bian, G., Blandin, S., Christensen, B.M., et al. (2007). Evolutionary dynamics of immune-related genes and pathways in disease-vector mosquitoes. Science *316*, 1738–1743.

Williams, M.J., Rodriguez, A., Kimbrell, D.A., and Eldon, E.D. (1997). The 18-wheeler mutation reveals complex antibacterial gene regulation in *Drosophila* host defense. EMBO J. *16*, 6120–6130.

Xu, Y., and Eissa, N.T. (2010). Autophagy in innate and adaptive immunity. Proc. Am. Thorac. Soc. *7*, 22–28.

Xu, Y., Jagannath, C., Liu, X.D., Sharafkhaneh, A., Kolodziejska, K.E., and Eissa, N.T. (2007). Toll-like receptor 4 is a sensor for autophagy associated with innate immunity. Immunity *27*, 135–144.

Yagi, Y., Nishida, Y., and Ip, Y.T. (2010). Functional analysis of Toll-related genes in *Drosophila*. Dev. Growth Differ. *52*, 771–783.

Yano, T., Mita, S., Ohmori, H., Oshima, Y., Fujimoto, Y., Ueda, R., Takada, H., Goldman, W.E., Fukase, K., Silverman, N., et al. (2008). Autophagic control of listeria through intracellular innate immune recognition in *Drosophila*. Nat. Immunol. *9*, 908–916.

Identification of a Primary Target of Thalidomide Teratogenicity

Takumi Ito,[1]* Hideki Ando,[2]* Takayuki Suzuki,[3,4] Toshihiko Ogura,[3] Kentaro Hotta,[2] Yoshimasa Imamura,[5] Yuki Yamaguchi,[2] Hiroshi Handa[1,2]†

Half a century ago, thalidomide was widely prescribed to pregnant women as a sedative but was found to be teratogenic, causing multiple birth defects. Today, thalidomide is still used in the treatment of leprosy and multiple myeloma, although how it causes limb malformation and other developmental defects is unknown. Here, we identified cereblon (CRBN) as a thalidomide-binding protein. CRBN forms an E3 ubiquitin ligase complex with damaged DNA binding protein 1 (DDB1) and Cul4A that is important for limb outgrowth and expression of the fibroblast growth factor Fgf8 in zebrafish and chicks. Thalidomide initiates its teratogenic effects by binding to CRBN and inhibiting the associated ubiquitin ligase activity. This study reveals a basis for thalidomide teratogenicity and may contribute to the development of new thalidomide derivatives without teratogenic activity.

During the late 1950s and early 1960s, thalidomide was sold as a sedative in over 40 countries and was often prescribed to pregnant women as a treatment for morning sickness. Before its teratogenic activity came to light and its use was discontinued, ~10,000 affected children were born from women taking thalidomide during pregnancy (*1*–*3*). Use of thalidomide during weeks 3 to 8 of gestation causes multiple birth defects such as limb, ear, cardiac, and gastrointestinal malformations (*1*–*3*). The limb malformations, known as phocomelia and amelia, are characterized, respectively, by severe shortening or complete absence of legs and/or arms, whereas the ear malformations lead to anotia, microtia, and hearing loss. Despite considerable effort, little is known about how these developmental defects are caused. Previous studies have suggested thalidomide-induced oxidative stress and its antiangiogenic action as a possible cause of teratogenicity (*4*, *5*). However, several important questions remain unanswered, such as what are direct targets of thalidomide and how the target molecules mediate its teratogenic effects.

Recently, thalidomide use has increased for the treatment of multiple myeloma and erythema nodosum leprosum, a painful complication of leprosy (*2*, *3*, *6*, *7*). Owing to its teratogenicity, however, thalidomide is used under strict control (*8*), and removal of its side effects is desirable for wider applications of this potentially useful drug. It is important to elucidate the molecular mechanism of thalidomide teratogenicity, especially to identify its molecular target(s), because such knowledge might allow rapid screening for potentially useful related compounds devoid of teratogenic activity. In this regard, we have been developing high-performance affinity beads that allow single-step affinity purification of drug target proteins from crude cell extracts (*9*). Here we show that cereblon (CRBN), a protein encoded by a candidate gene for mild mental retardation, is a primary target of thalidomide teratogenicity.

Binding of thalidomide to CRBN and DDB1. To purify thalidomide-binding proteins, we performed affinity purification using ferrite-glycidyl methacrylate (FG) beads (*9*). The carboxylic thalidomide derivative FR259625 was covalently conjugated to the beads (fig. S1) and incubated with human HeLa cell extracts (*10*). After extensive washing, bound proteins were eluted with free thalidomide, and the eluate fractions were subjected to SDS gel electrophoresis and silver staining. Two polypeptides were specifically eluted (Fig. 1A, lane 3). When free thalidomide was added to extracts before incubation with the beads, the yields of these proteins were reduced (Fig. 1A, lane 4), which suggested that these proteins specifically interact with thalidomide. The 127- and 55-kD proteins were therefore subjected to proteolytic digestion and tandem mass spectrometry and were identified as CRBN and damaged DNA binding protein 1 (DDB1), respectively (table S1). Identities of these proteins were confirmed by immunoblotting (Fig. 1A). CRBN and DDB1 were isolated similarly as thalidomide-binding proteins from various cell types (fig. S2). To determine whether this interaction is direct, we used purified recombinant proteins. FLAG-tagged CRBN, but not V5 (GKPIPNPLLGLDST) (*11*) epitope- and histidine (His)–tagged DDB1, bound to thalidomide beads (Fig. 1B). We therefore asked whether DDB1 binds to thalidomide beads through its interaction with CRBN. As expected, DDB1 was coprecipitated with FLAG- and hemagglutinin (HA) epitope–tagged (FH-) CRBN (Fig. 1C) and was not affinity-purified from CRBN-depleted 293T cells (fig.

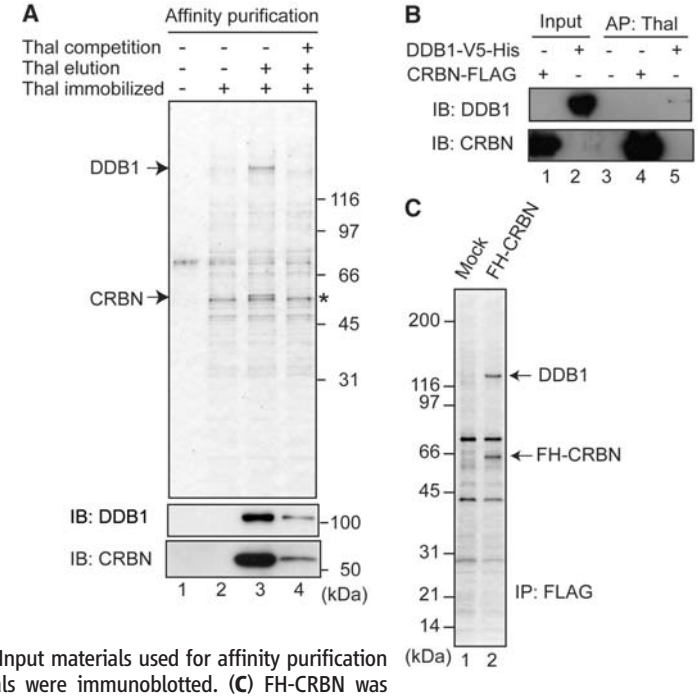

Fig. 1. Thalidomide binds to CRBN and DDB1. (**A**) Thalidomide (Thal)-binding proteins were purified from HeLa cell extracts by using thalidomide-immobilized (+) or control (–) beads. Where indicated, bound proteins were eluted with free thalidomide. As indicated, 0.3 mM thalidomide was added to extracts before incubation with the beads. Eluted proteins were analyzed by silver staining (top) or immunoblotting (IB) (bottom). Asterisk indicates nonspecific signal. (**B**) Purified recombinant CRBN-FLAG and DDB1-V5-His were, respectively, incubated with thalidomide beads. Input materials used for affinity purification (AP) and bound materials were immunoblotted. (**C**) FH-CRBN was immunoprecipitated (IP) from 293T cells stably expressing FH-CRBN or from control cells, followed by SDS gel electrophoresis and silver staining.

[1]Integrated Research Institute, Tokyo Institute of Technology, Yokohama 226-8503, Japan. [2]Graduate School of Bioscience and Biotechnology, Tokyo Institute of Technology, Yokohama 226-8501, Japan. [3]Institute of Development, Aging and Cancer, Tohoku University, Sendai 980-8575, Japan. [4]Precursory Research for Embryonic Science and Technology, Japan Science and Technology Agency (JST), Saitama 332-0012, Japan. [5]Drug Discovery Research, Astellas Pharma Inc., Ibaraki 305-8585, Japan.

*These authors contributed equally to this work.
†To whom correspondence should be addressed. E-mail: handa.h.aa@m.titech.ac.jp

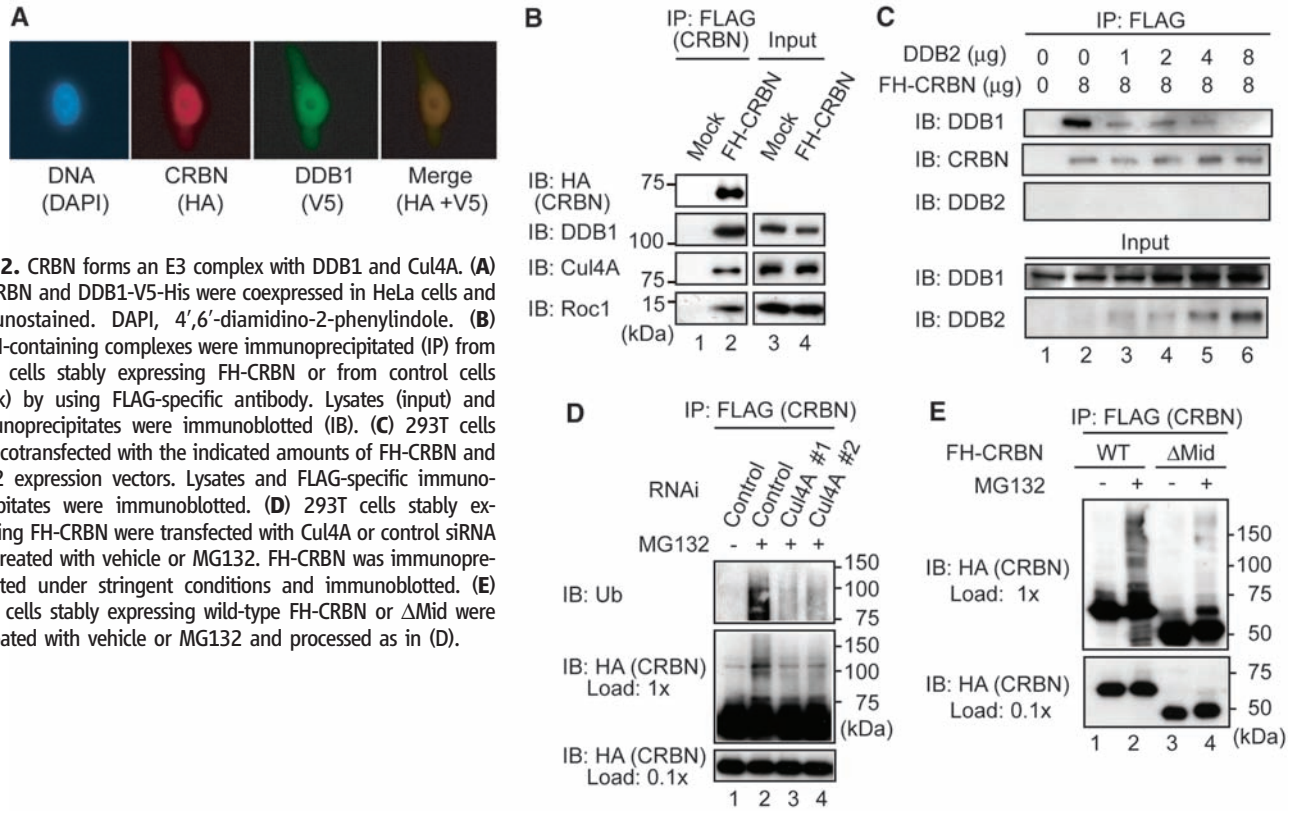

Fig. 2. CRBN forms an E3 complex with DDB1 and Cul4A. (**A**) FH-CRBN and DDB1-V5-His were coexpressed in HeLa cells and immunostained. DAPI, 4′,6′-diamidino-2-phenylindole. (**B**) CRBN-containing complexes were immunoprecipitated (IP) from 293T cells stably expressing FH-CRBN or from control cells (mock) by using FLAG-specific antibody. Lysates (input) and immunoprecipitates were immunoblotted (IB). (**C**) 293T cells were cotransfected with the indicated amounts of FH-CRBN and DDB2 expression vectors. Lysates and FLAG-specific immunoprecipitates were immunoblotted. (**D**) 293T cells stably expressing FH-CRBN were transfected with Cul4A or control siRNA and treated with vehicle or MG132. FH-CRBN was immunoprecipitated under stringent conditions and immunoblotted. (**E**) 293T cells stably expressing wild-type FH-CRBN or ΔMid were incubated with vehicle or MG132 and processed as in (D).

S3A), which led us to conclude that thalidomide interacts directly with CRBN and indirectly with DDB1 through its interaction with CRBN. The equilibrium dissociation constant of the CRBN-thalidomide interaction was calculated to be 8.5 nM (*10*). Moreover, CRBN did not bind to phthalimide, a nonteratogenic analog of thalidomide (*12*), which substantiated the high affinity and specificity of the CRBN-thalidomide interaction (fig. S3B).

Formation of an E3 complex by CRBN, DDB1, and Cul4A. Human *CRBN* was originally identified as a candidate gene for autosomal recessive mild mental retardation and encodes a 442–amino acid protein that is highly conserved from plants to humans (*13*). Although CRBN was reported to interact with DDB1 in a recent proteomic analysis (*14*), the functional relevance of this interaction remains unclear. Consistent with the apparently stoichiometric interaction of CRBN and DDB1 (Fig. 1C), these proteins are colocalized mainly in the nucleus, but also in the cytoplasm (Fig. 2A). DDB1 is a component of E3 ubiquitin ligase complexes containing Cullin 4 (Cul4A or Cul4B), regulator of cullins 1 (Roc1), and a substrate receptor (*15*, *16*). In principle, the function of E3 ubiquitin ligases is to direct the polyubiquitination of substrate proteins by a specifically interacting ubiquitin-conjugating enzyme (E2) (*17*, *18*). Cul4 is thought to play a scaffold function, whereas Roc1 has a RING finger domain that associates with the E2 ubiquitin-conjugating enzyme. Substrate receptors, such as DDB2, CSA, and CDT2, directly bind to specific substrates and mediate their ubiquitination (*15*, *19*, *20*). We examined whether CRBN interacts with other components of the E3 complex and found that Cul4A and Roc1 were indeed coprecipitated with FH-CRBN (Fig. 2B). If CRBN functions as a substrate receptor of a Cul4-DDB1 E3 complex, it would be expected to compete for binding to DDB1 with other substrate receptor subunits, such as DDB2. Consistent with this, the amount of DDB1 coprecipitated with FH-CRBN was reduced in the presence of increasing amounts of coexpressed DDB2 (Fig. 2C). Although thalidomide can induce oxidative DNA damage (*4*), CRBN is likely to function independently of the DDB2-mediated DNA damage response pathway [see supporting online material (SOM) text].

We then examined whether the CRBN complex actually has E3 ubiquitin ligase activity. Because substrate receptors and Cul4 are known to undergo autoubiquitination in vitro in the absence of their specific substrates (*15*, *16*), in vitro ubiquitination assays were performed using purified protein components. Indeed, intrinsic ubiquitination activity was observed in the presence of the CRBN complex (fig. S4). We then examined whether CRBN is autoubiquitinated in cells. For this, CRBN was affinity-purified from 293T cells expressing FH-CRBN in the presence or absence of the proteasome inhibitor MG132. Autoubiquitination of FH-CRBN was detected in the presence of MG132, and its ubiquitination was abrogated by small interfering RNA (siRNA)–mediated depletion (knockdown) of Cul4A (Fig. 2D, fig. S5A, and table S2). Knockdown of DDB1 led to a substantial reduction of the CRBN protein level (fig. S5B), and it was not possible to determine the effect of DDB1 knockdown on CRBN ubiquitination. Nevertheless, this finding suggests that DDB1 and CRBN are functionally linked.

To further investigate the role of DDB1 in CRBN function, we obtained a CRBN mutant deficient in DDB1 binding. Mutational analysis revealed that deletion of amino acids 187 to 260 of CRBN (ΔMid) abolishes its interaction with DDB1 (fig. S6). ΔMid was therefore stably expressed in 293T cells and examined for its ubiquitination after MG132 treatment. Ubiquitination of ΔMid was reduced compared with wild-type CRBN (Fig. 2E). Collectively, these findings suggest that CRBN is a subunit of a functional E3 ubiquitin ligase complex and undergoes autoubiquitination in a Cul4A- and DDB1-dependent manner.

Inhibition of CRBN function by thalidomide. To investigate the structural basis of the CRBN-thalidomide interaction and its functional significance, we wished to obtain a CRBN point mutant that does not bind to thalidomide but is assembled into a functional E3 complex. Using a series of deletion mutants, we mapped its thalidomide-binding region to the C-terminal 104 amino acids, which corresponds to the most highly conserved region of the protein (figs. S7 and S8). Assuming that evolutionarily conserved residues may be important for thalidomide binding, we constructed a series of point mutants, and two point

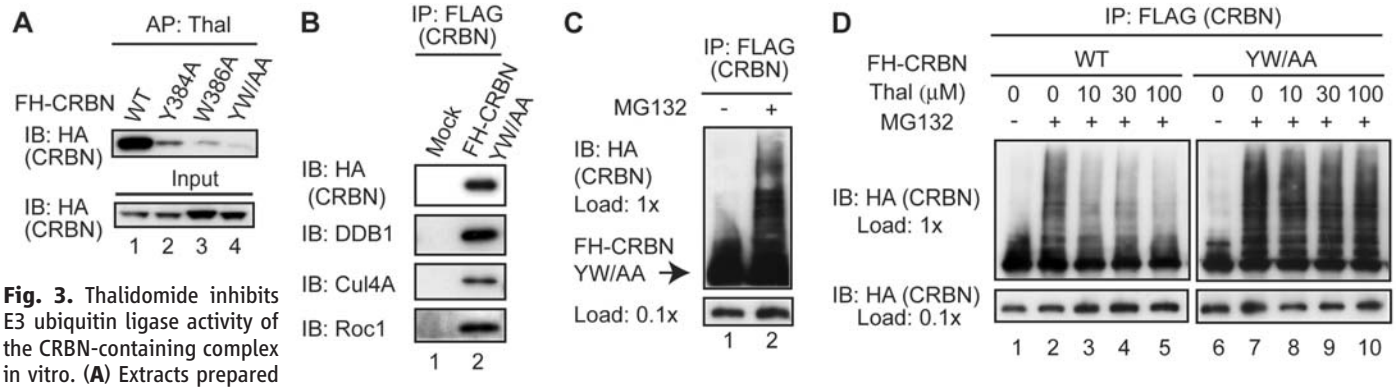

Fig. 3. Thalidomide inhibits E3 ubiquitin ligase activity of the CRBN-containing complex in vitro. (**A**) Extracts prepared from 293T cells overexpressing FH-CRBN or one of its mutants were incubated with thalidomide-immobilized beads, and lysates (input) and affinity-purified (AP) materials were immunoblotted (IB). (**B**) 293T cells stably expressing FH-CRBN$^{YW/AA}$ were subjected to FLAG-specific antibody immunoprecipitation (IP) and immunoblotting. (**C** and **D**) 293T cells stably expressing FH-CRBN or FH-CRBN$^{YW/AA}$ were processed as in Fig. 2E. In (D), cells were treated with the indicated concentrations of thalidomide for 4 hours before harvest.

mutants, Y384A and W386A, were found to be defective for thalidomide binding (Fig. 3A) (*11*). Moreover, the double point mutant Y384A/W386A (CRBN$^{YW/AA}$) had extremely low thalidomide-binding activity. We then asked whether CRBN$^{YW/AA}$ is functionally active in cells. The subcellular localization of the mutant was indistinguishable from wild-type CRBN (fig. S7C). Moreover, CRBN$^{YW/AA}$ was coprecipitated with DDB1, Cul4A, and Roc1 (Fig. 3B) and was autoubiquitinated after MG132 treatment (Fig. 3C), which demonstrated that CRBN$^{YW/AA}$ is assembled into a complete E3 ubiquitin ligase complex.

We examined possible effects of thalidomide on ubiquitination by treating 293T cells stably expressing FH-CRBN or FH-CRBN$^{YW/AA}$ with MG132 and thalidomide at similar or higher concentrations relative to the therapeutic doses used in humans (*21*). Autoubiquitination of wild-type CRBN was inhibited by thalidomide in a concentration-dependent manner, whereas autoubiquitination of CRBN$^{YW/AA}$ was not affected by thalidomide even at the highest concentration used (Fig. 3D). Together, these results suggest that thalidomide inhibits E3 function of the CRBN-containing complex by directly binding to CRBN.

CRBN as an in vivo target of thalidomide. Next, we investigated a possible role of CRBN in thalidomide teratogenicity in animal models. Thalidomide is teratogenic in rabbits and chicks, but not in mice and rats (*1*–*3*). We first used zebrafish as a model system because (i) the rapid progress of development of zebrafish can be monitored in real time because of the transparency of the embryo, (ii) knockdown of genes of interest can be carried out easily (*22*), and (iii) zebrafish are suitable for pharmacotoxicological studies (*23*). Given that thalidomide was recently shown to inhibit angiogenesis in zebrafish embryos (*24*), we reasoned that zebrafish might be susceptible to other activities of thalidomide.

To examine the effects of thalidomide on zebrafish development, we transferred dechorionated embryos to media containing different concentrations of thalidomide at 2 hours post fertilization (hpf) and allowed them to develop for 3 days. It was immediately apparent that in thalidomide-treated embryos, development of pectoral fins and otic vesicles was disturbed, whereas other aspects of development were not generally affected (Fig. 4, A and B, and fig. S9). More specifically, formation of the proximal endoskeletal disc of the pectoral fin was severely inhibited at 75 hpf (Fig. 4A), and otic vesicle size was significantly reduced at 30 hpf (Fig. 4B and fig. S11). Pectoral fin malformations were already apparent at 48 hpf (Fig. 5, C and D). More detailed phenotypes induced by thalidomide are described in the SOM text. Recent studies have suggested that development of pectoral fins and otic vesicles in teleosts share common molecular pathways with that of tetrapod limbs and ears (*25*–*27*).

Zebrafish have a *CRBN* orthologous gene which we call *zcrbn*, whose product has ~70% identity to human CRBN (fig. S8). We first examined the expression pattern of *zcrbn* mRNA and found that the gene is highly expressed in the brain, head vasculature, otic vesicles, and developing pectoral fins at 30 and 48 hpf (fig. S12). zCrbn interacts with DDB1 and is affinity-purified from zebrafish embryos as a major interactor with thalidomide (fig.

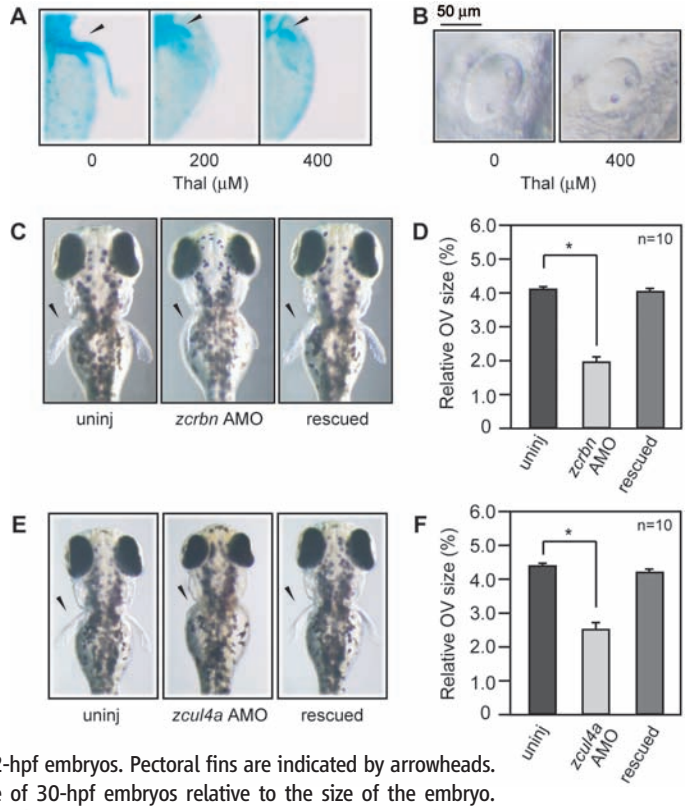

Fig. 4. Thalidomide treatment or down-regulation of the CRBN complex causes similar developmental defects in zebrafish. (**A** and **B**) Zebrafish embryos were allowed to develop in media containing the indicated concentrations of thalidomide. (A) Embryos at 75 hpf were fixed and stained with Alcian blue. Pectoral fins are indicated by arrowheads. (B) Close-up view of otic vesicles of 30-hpf live embryos. (**C** and **D**) Where indicated, *zcrbn* AMO was injected with (rescued) or without *zcrbn* mRNA into one-cell stage embryos. (**E** and **F**) Where indicated, *zcul4a* AMO was injected with or without *zcul4a* mRNA into one-cell stage embryos. (C and E) Dorsal views of pectoral fins of 72-hpf embryos. Pectoral fins are indicated by arrowheads. (D and F) Otic vesicle size of 30-hpf embryos relative to the size of the embryo. Representative raw data are shown in fig. S14. *$P < 0.001$. uninj, uninjected.

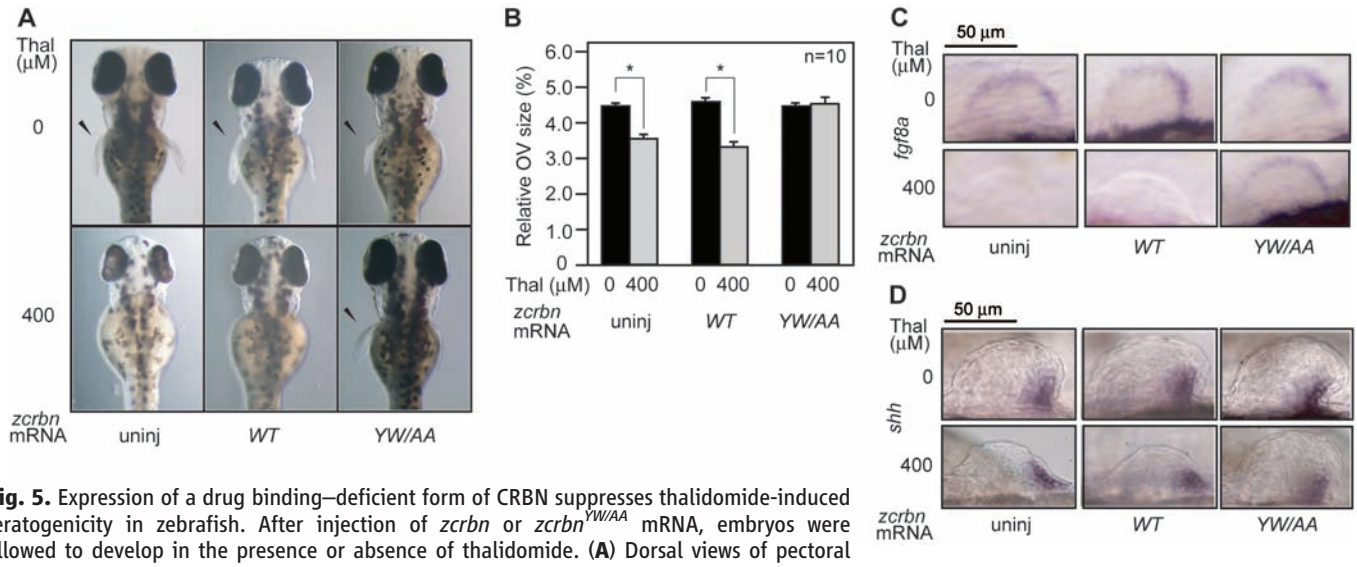

Fig. 5. Expression of a drug binding–deficient form of CRBN suppresses thalidomide-induced teratogenicity in zebrafish. After injection of *zcrbn* or *zcrbn*$^{YW/AA}$ mRNA, embryos were allowed to develop in the presence or absence of thalidomide. (**A**) Dorsal views of pectoral fins of 72-hpf embryos. Fins are indicated by arrowheads. (**B**) Otic vesicle size of 30-hpf embryos relative to the size of the embryo. *$P < 0.001$. (**C** and **D**) Embryos at 48 hpf were subjected to hybridization with antisense probes for *fgf8a* or *shh*. Close-up views of fin buds are shown. uninj, uninjected.

S13), which suggests that the findings of our cell culture studies are valid in zebrafish. Hence, the function of zCrbn during early development was examined. Embryos injected with an antisense morpholino oligonucleotide (AMO) for *zcrbn* exhibited specific defects in fin and otic vesicle development (Fig. 4, C and D, and figs. S9 to S11 and S14), phenotypes similar to those of thalidomide-treated embryos. For example, the size of otic vesicles was reduced by half in the knockdown embryos (Fig. 4D). These defects were rescued by coinjection of *zcrbn* mRNA (Fig. 4, C and D, and figs. S9 to S11 and S14).

The above findings suggested an interesting possibility that thalidomide exerts teratogenic effects by inhibiting zCrbn function. If so, its teratogenic effects might be reversed by overexpression of a functionally active, thalidomide binding–defective form of zCrbn. To test this idea, we used zCrbn carrying Y374A and W376A mutations, which correspond to Y384A and W386A mutations in human CRBN. zCrbn$^{YW/AA}$ had extremely low thalidomide-binding activity (fig. S13C). In the absence of thalidomide, overexpression of zCrbn or zCrbn$^{YW/AA}$ had no discernible effect on fin and otic vesicle development (Fig. 5 and figs. S9 to S11). As we have already seen in Fig. 4, thalidomide treatment significantly reduced otic vesicle size ($P < 0.001$, Mann-Whitney U test) (Fig. 5B and fig. S11). Thalidomide treatment of embryos overexpressing wild-type zCrbn similarly reduced otic vesicle size ($P < 0.001$). However, thalidomide treatment of embryos overexpressing zCrbn$^{YW/AA}$ did not affect otic vesicle size significantly ($P = 0.59$). Thalidomide-induced pectoral fin malformations were also rescued by overexpression of zCrbn$^{YW/AA}$ (Fig. 5A and fig. S10), which demonstrated that thalidomide exerts teratogenic effects by binding to CRBN and inhibiting its function.

Molecular mechanism of thalidomide teratogenicity. As the connection between thalidomide and CRBN was established, we then examined whether the CRBN-containing E3 complex is involved in thalidomide teratogenicity, by down-regulating the zebrafish homolog of Cul4A (zCul4a). *zcul4a* mRNA is abundantly expressed in the brain and pectoral fins (fig. S12). As expected, microinjection of AMO for *zcul4a* caused similar defects in otic vesicles and pectoral fins, and these phenotypes were rescued by coinjection of *zcul4a* mRNA (Fig. 4, E and F, and figs. S9 to S11 and S14). Nevertheless, phenotypic similarities between zCrbn and zCul4A knockdown embryos may be just coincidental. To rule out this possibility, we examined the importance of the physical interaction between CRBN and DDB1 in vivo, by using zCrbn$^{\Delta Mid\ YW/AA}$. As expected, DDB1 and thalidomide did not bind to this mutant, and thalidomide-induced developmental defects were not rescued by its overexpression (fig. S15). These results suggest that the CRBN-containing E3 ubiquitin ligase complex plays a crucial role in fin and otic vesicle development and is a target of thalidomide.

To obtain a clue to the pathway(s) downstream of thalidomide and CRBN, we examined expression of key signaling molecules during pectoral fin development. Sonic hedgehog (Shh) is expressed in the zone of polarizing activity (ZPA) and is responsible for anteroposterior patterning of limbs (*28*), whereas fibroblast growth factor (fgf) 8 is expressed in the apical ectodermal ridge (AER) of limbs and is responsible for limb outgrowth along the proximodistal axis (*29*, *30*). In thalidomide-treated 48-hpf embryos, *fgf8a* expression in the AER was severely reduced or absent (Fig. 5C), whereas *shh* expression in the ZPA was affected negligibly (Fig. 5D). In addition, *fgf8a* expression was restored by injection of *zcrbn*$^{YW/AA}$ mRNA (Fig. 5C). Knockdown of zCrbn or zCul4a also resulted in a reduction of *fgf8a* expression in the AER, whereas it had little effect on *shh* expression in the ZPA (fig. S14). Thus, an inhibitor of fgf8 production is a possible downstream target of thalidomide and the CRBN-containing E3 complex.

Conserved role for CRBN in zebrafish and chicks. Finally, in order to validate our findings, we used chicks, well-established model organisms for studying thalidomide teratogenicity. As reported previously (*12*, *31*), exposure to thalidomide resulted in the complete absence of a forelimb at a high incidence (Fig. 6A and fig. S16). Overexpression of human CRBN$^{YW/AA}$, but not wild-type CRBN, in the forelimb field remarkably reduced thalidomide sensitivity (Fig. 6A and fig. S16). Expression of *fgf8* and *fgf10* was then examined. Fgf10 is also an important regulator of proximodistal limb patterning and is normally expressed in the mesoderm beneath the AER (Fig. 6B). Thalidomide down-regulated *fgf10* expression in the mesoderm and, perhaps to a lesser extent, *fgf8* expression in the AER, and their expression was restored by overexpression of CRBN$^{YW/AA}$ (Fig. 6B). These results, together with the finding that chick CRBN binds to thalidomide and DDB1 (fig. S17), suggest that the developmental role of CRBN is conserved in fins and limbs.

Discussion. The mechanism of action of thalidomide appears to be multifaceted, but is not fully understood. The immunomodulatory and antiangiogenic activities of thalidomide have been proposed to be partly responsible for its teratogenic activity, as well as its therapeutic value in the treatment of leprosy and multiple myeloma (*2*, *3*, *6*, *7*). In this respect, thalidomide is known to inhibit the production of some cytokines such as tumor necrosis factor–α and vascular endothelial growth factor (*32*, *33*). Thalidomide is also capable of inducing apoptosis and producing reactive oxygen species (*3*, *4*). Despite such accumulating data, little is known about direct

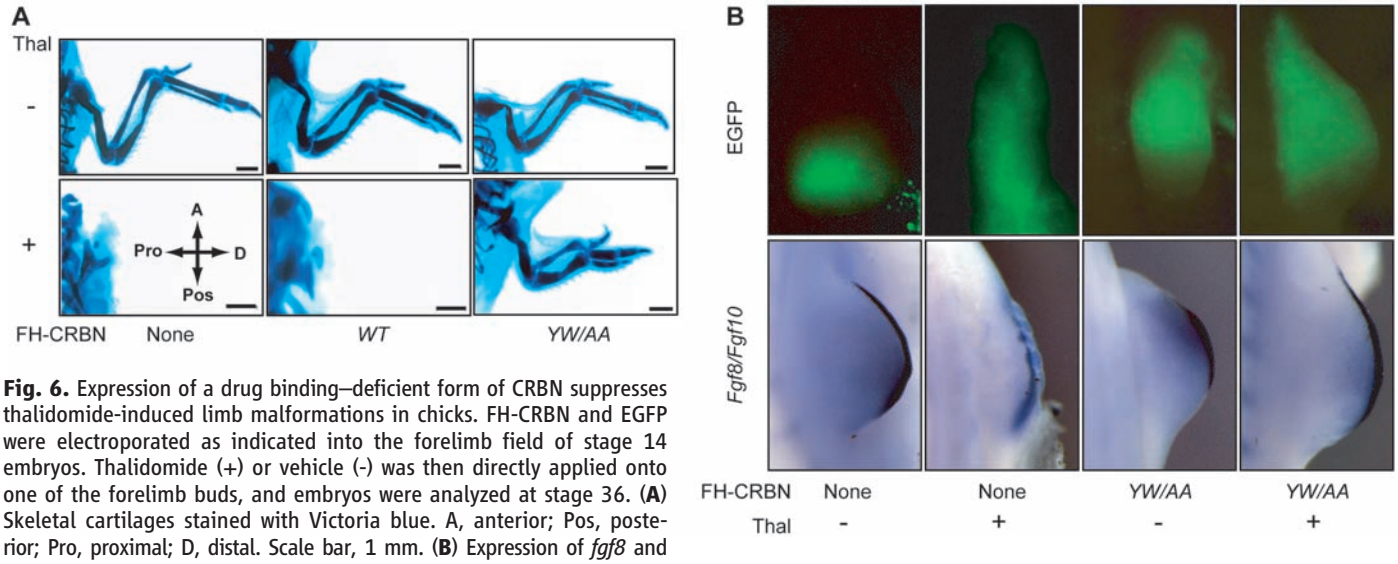

Fig. 6. Expression of a drug binding–deficient form of CRBN suppresses thalidomide-induced limb malformations in chicks. FH-CRBN and EGFP were electroporated as indicated into the forelimb field of stage 14 embryos. Thalidomide (+) or vehicle (-) was then directly applied onto one of the forelimb buds, and embryos were analyzed at stage 36. (**A**) Skeletal cartilages stained with Victoria blue. A, anterior; Pos, posterior; Pro, proximal; D, distal. Scale bar, 1 mm. (**B**) Expression of *fgf8* and *fgf10* visualized by in situ hybridization. EGFP marks area of electroporation.

molecular targets of thalidomide. Here we provided several lines of evidence that CRBN is a primary target of thalidomide teratogenicity. Because overexpression of the thalidomide-insensitive form of CRBN rescued the effects of thalidomide largely, if not entirely, in zebrafish and chicks, CRBN is thought to play an important role as an upstream mediator of thalidomide action at least in these species. Whereas CRBN is ubiquitously expressed in humans, thalidomide exerts tissue-specific effects. Evidently, CRBN is necessary, but not sufficient, for thalidomide teratogenicity, and downstream components are likely to contribute to the tissue-specific effects of thalidomide (see SOM text).

The finding that fgf8 is a downstream target of thalidomide and CRBN fits well with a previous report, in which a similar effect of thalidomide on *fgf8* expression was described in rabbits, another sensitive species (*34*). In developing chick limb buds, thalidomide was shown to up-regulate expression of a subset of bone morphogenetic protein (BMP) family genes and to induce apoptosis (*12*). Coincidentally, mouse BMPs were shown to inhibit *fgf8* expression and to induce apoptosis in the AER (*35*). Thus, CRBN appears to be a missing link between thalidomide and these key developmental regulators.

However, this study does not rule out other mechanisms of thalidomide action, particularly in mammals. Thalidomide-induced oxidative stress is thought to occur through the direct formation of reactive oxygen species (*4*) and is therefore clearly a CRBN-independent process. Second, a recent study suggested antiangiogenic activity of thalidomide as a primary cause of chick limb malformations, demonstrating that thalidomide-induced inhibition of vasculogenesis precedes inhibition of *fgf8* expression and cell death in limb buds (*31*). By contrast, our data suggest that, in zebrafish, inhibition of vasculogenesis follows thalidomide-induced morphological and transcriptional changes in pectoral fin buds (fig. S18 and SOM text), which implies that the sequence of events induced by thalidomide is different in these organisms. These observations are concordant with the common view of species differences in thalidomide action (see SOM for further discussion on the species differences). Another point to consider is the fact that thalidomide is rapidly hydrolyzed or metabolized to more than a dozen products in vitro and in vivo (*2*, *21*, *36*). Thalidomide and its products may have the same or different molecular target(s) (see SOM text).

Our findings suggest that thalidomide exerts teratogenic effects, at least in part, by binding to CRBN and inhibiting the associated ubiquitin ligase activity (fig. S19). We speculate that control of ubiquitin-dependent proteolysis by thalidomide and CRBN leads to abnormal regulation of the BMP and fgf8 signaling pathways and of developmental programs that require their normal functions. Incidentally, many E3 ubiquitin ligases are known to target developmental and/or transcriptional regulators and to control developmental programs (*37*, *38*). There are, however, a number of unanswered questions, such as: What are the substrates of CRBN E3 ubiquitin ligase? How does thalidomide inhibit the ubiquitination of CRBN in the ligase complex? How might this pathway be interconnected to the other pathways targeted by thalidomide? These issues need to be addressed to fully appreciate the model. Last, but not least, because thalidomide is now used for the treatment of multiple myeloma and leprosy, identification of its direct target may allow rational design of more effective thalidomide derivatives without teratogenic activity (see SOM text).

References and Notes

1. M. T. Miller, K. Strömland, *Teratology* **60**, 306 (1999).
2. M. Melchert, A. List, *Int. J. Biochem. Cell Biol.* **39**, 1489 (2007).
3. J. Knobloch, U. Rüther, *Cell Cycle* **7**, 1121 (2008).
4. T. Parman, M. J. Wiley, P. G. Wells, *Nat. Med.* **5**, 582 (1999).
5. R. J. D'Amato, M. S. Loughnan, E. Flynn, J. Folkman, *Proc. Natl. Acad. Sci. U.S.A.* **91**, 4082 (1994).
6. J. Sheskin, *Clin. Pharmacol. Ther.* **6**, 303 (1965).
7. S. Singhal *et al.*, *N. Engl. J. Med.* **341**, 1565 (1999).
8. J. B. Zeldis, B. A. Williams, S. D. Thomas, M. E. Elsayed, *Clin. Ther.* **21**, 319 (1999).
9. S. Sakamoto, Y. Kabe, M. Hatakeyama, Y. Yamaguchi, H. Handa, *Chem. Rec.* **9**, 66 (2009).
10. Materials and methods and additional text are available as supporting information on *Science* Online.
11. Single-letter abbreviations for the amino acid residues used in this research article are as follows: A, Ala; C, Cys; D, Asp; E, Glu; F, Phe; G, Gly; H, His; I, Ile; K, Lys; L, Leu; M, Met; N, Asn; P, Pro; Q, Gln; R, Arg; S, Ser; T, Thr; V, Val; W, Trp; and Y, Tyr.
12. J. Knobloch, J. D. Shaughnessy Jr., U. Rüther, *FASEB J.* **21**, 1410 (2007).
13. J. J. Higgins, J. Pucilowska, R. Q. Lombardi, J. P. Rooney, *Neurology* **63**, 1927 (2004).
14. S. Angers *et al.*, *Nature* **443**, 590 (2006).
15. R. Groisman *et al.*, *Cell* **113**, 357 (2003).
16. F. Ohtake *et al.*, *Nature* **446**, 562 (2007).
17. C. M. Pickart, *Cell* **116**, 181 (2004).
18. M. D. Petroski, R. J. Deshaies, *Nat. Rev. Mol. Cell Biol.* **6**, 9 (2005).
19. K. Sugasawa *et al.*, *Cell* **121**, 387 (2005).
20. J. Jin, E. E. Arias, J. Chen, J. W. Harper, J. C. Walter, *Mol. Cell* **23**, 709 (2006).
21. M. E. Franks, G. R. Macpherson, W. D. Figg, *Lancet* **363**, 1802 (2004).
22. A. Nasevicius, S. C. Ekker, *Nat. Genet.* **26**, 216 (2000).
23. M. B. Veldman, S. Lin, *Pediatr. Res.* **64**, 470 (2008).
24. T. Yabu *et al.*, *Blood* **106**, 125 (2005).
25. M. Tanaka *et al.*, *Nature* **416**, 527 (2002).
26. M. C. Davis, R. D. Dahn, N. H. Shubin, *Nature* **447**, 473 (2007).
27. A. Streit, *J. Anat.* **199**, 99 (2001).
28. R. D. Riddle, R. L. Johnson, E. Laufer, C. Tabin, *Cell* **75**, 1401 (1993).
29. A. M. Moon, M. R. Capecchi, *Nat. Genet.* **26**, 455 (2000).
30. M. Lewandoski, X. Sun, G. R. Martin, *Nat. Genet.* **26**, 460 (2000).
31. C. Therapontos, L. Erskine, E. R. Gardner, W. D. Figg, N. Vargesson, *Proc. Natl. Acad. Sci. U.S.A.* **106**, 8573 (2009).
32. A. L. Moreira *et al.*, *J. Exp. Med.* **177**, 1675 (1993).
33. D. Gupta *et al.*, *Leukemia* **15**, 1950 (2001).
34. J. M. Hansen, S. G. Gong, M. Philbert, C. Harris, *Dev. Dyn.* **225**, 186 (2002).
35. S. Pajni-Underwood, C. P. Wilson, C. Elder, Y. Mishina, M. Lewandoski, *Development* **134**, 2359 (2007).
36. F. Chung *et al.*, *Clin. Cancer Res.* **10**, 5949 (2004).

37. Y. Cang *et al.*, *Cell* **127**, 929 (2006).
38. Y. Cang *et al.*, *Proc. Natl. Acad. Sci. U.S.A.* **104**, 2733 (2007).
39. We thank T. Wada, S. Sakamoto, and S. Ishihara for discussions; P. Raychaudhuri, T. Matsunaga, S. Krauss, B. Thisse, A. Kawakami, S. Noji, J. Izpisua-Belmonte, K. Kawakami, and J. Yamauchi for valuable reagents; Y. Tsuboi for technical support; and P. Sharp and A. Berk for comments on this manuscript. This work was supported by Special Coordination Funds for Promoting Science and Technology from JST, by the Global COE (Center of Excellence) Program from the Japan Ministry of Education, Culture, Sports, Science, and Technology (MEXT), and by a grant for Research and Development Projects in Cooperation with Academic Institutions from the New Energy and Technology Development Organization (H.H. and H.A.). This work was also supported by grants-in-aid for Scientific Research (20370084 to T.O.) and for Young Scientists (21770226 to T.S.) from MEXT and by the Precursory Research for Embryonic Science and Technology program from JST (T.S.). T.I. was a Japan Society for the Promotion of Science Research Fellow. An application for a patent has been filed in the Japan Patent Office.

Supporting Online Material
www.sciencemag.org/cgi/content/full/327/5971/1345/DC1
Materials and Methods
SOM Text
Figs. S1 to S19
Tables S1 and S2
References

5 June 2009; accepted 10 February 2010
10.1126/science.1177319

REPORTS

Variations in the Sun's Meridional Flow over a Solar Cycle

David H. Hathaway[1]* and Lisa Rightmire[2]

The Sun's meridional flow is an axisymmetric flow that is generally directed from its equator toward its poles at the surface. The structure and strength of the meridional flow determine both the strength of the Sun's polar magnetic field and the intensity of sunspot cycles. We determine the meridional flow speed of magnetic features on the Sun using data from the Solar and Heliospheric Observatory. The average flow is poleward at all latitudes up to 75°, which suggests that it extends to the poles. It was faster at sunspot cycle minimum than at maximum and substantially faster on the approach to the current minimum than it was at the last solar minimum. This result may help to explain why this solar activity minimum is so peculiar.

The Sun's meridional flow has been difficult to measure (*1*). Its amplitude (10 to 20 m s^{-1}) is more than an order of magnitude weaker than that of the other major flows on the surface of the Sun (granulation ~3000 m s^{-1}, supergranulation ~300 m s^{-1}, and differential rotation ~170 m s^{-1}). In the past, this has led to reports of vastly different flow speeds and directions (*2*–*5*). Despite its weakness, the meridional flow plays a key role in the magnetic evolution of the Sun's surface. It transports magnetic elements that, when carried to the poles, reverse the magnetic polarity of the poles and build up polar fields of opposite polarity after each sunspot cycle maximum. Models of this magnetic flux transport process (*6*–*8*) have employed a variety of substantially different flow profiles. The fidelity of these flux transport models is important because they are used in climate change studies (*9*, *10*) to estimate the total irradiance of the Sun over the past century. The meridional flow is also key to flux transport dynamo models that have been used to predict the amplitude of Solar Cycle 24 (*11*, *12*). An obvious conflict between the surface flux transport models (*6*–*10*) and the flux transport dynamo models (*11*, *12*) is found in their sensitivity to the strength of the meridional flow. A stronger meridional flow produces weaker polar fields in the surface flux transport models, whereas the same flow produces stronger polar fields (and shorter sunspot cycles) in the flux transport dynamos. Solar Cycle 23 (1996 to 2008) provides an interesting problem for all of these models. The strength of the polar fields produced after cycle maximum in 2000–2001 was only about half that seen in the previous three solar cycles (*13*). Furthermore, cycle 24 started much later than average. The late start for cycle 24 has left behind a long quiet minimum unlike any in the past 100 years.

We measured the Sun's meridional flow to determine its variability over Solar Cycle 23 by following the motions of the small magnetic elements that populate the entire surface of the Sun. These are precisely the elements whose motions are modeled in both the surface flux transport models and the flux transport dynamo models. Motions of sunspots, and even the plasma at the surface, are known to differ from those of the small magnetic elements (*1*–*5*). The data we used have been acquired by the Michelson Doppler Imager (MDI) on the European Space Agency (ESA)/National Aeronautics and Space Administration (NASA) Solar and Heliospheric Observatory (SOHO). MDI produces images of the line-of-sight magnetic field across the visible solar disc every 96 min. This is done by measuring differences in circular polarization on either side of a spectral absorption line caused by traces of nickel in the Sun's atmosphere (*14*). We measured the displacement of the magnetic elements by comparing their positions at 8-hour (5-image) intervals from May 1996 to June 2009. The 1024-by-1024 pixel magnetic images were mapped onto a 1024-by-1024 grid in heliographic latitude and longitude from the central meridian. This mapping accounts for changes in the position angle of the Sun's rotation axis relative to the spacecraft's vertical axis, changes in the tilt angle of the Sun's rotation axis toward or away from the spacecraft, and changes in perspective at different distances from the Sun. Because sunspots have very different proper motions (*4*) and produce localized outflows (*15*), we removed sunspots and their immediate surroundings by masking all pixels with measured absolute field strengths greater than 500 Gauss and all contiguous pixels of the same polarity with absolute field strengths above 100 Gauss. Displacements in longitude and

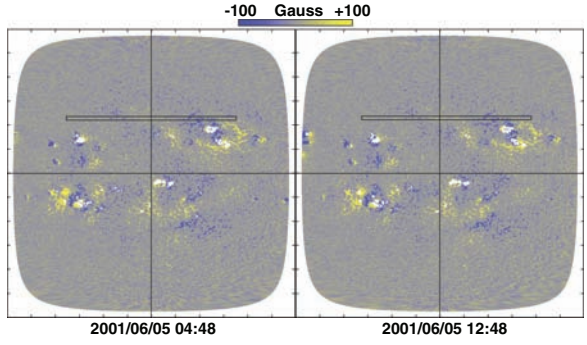

Fig. 1. Magnetic element motion. A pair of masked magnetic maps from 5 June 2001 that were obtained 8 hours apart are shown here with blue representing negative magnetic polarity and yellow representing positive magnetic polarity. The tick marks around the borders are at 15° intervals in latitude and in longitude from the central meridian. The masked-out sunspot areas are evident as white patches. The strongest correlation for the outlined strip of pixels in the earlier map (**left**) is calculated to occur for a shift of 23.7 pixels in longitude and 0.4 pixels in latitude for a similar strip in the later map (**right**).

[1]NASA Marshall Space Flight Center, Huntsville, AL 35812, USA. [2]University of Memphis, Memphis, TN 38152, USA.

*To whom correspondence should be addressed. E-mail: david.hathaway@nasa.gov